CHAPTER ONE

INTRODUCTION

1.1 Introduction

In nowadays the production of Silicon solar cells, the registered efficiency is a bout of 24 % (Thorstensen, 2013). General aspect of several high-efficiency for solar cell concepts they require some form of its local processing, that is lab-scale cells has been enabled by photolithography. Photolithography, commonly considered incompatible with the very high throughput demanded by the solar cell industry. Laser has the capabilities to be used in industrial scale local processing due to its an excellent spatial resolution and translational control, which provides similar local processing capabilities that, has simpler processes, and may as such open for industrial scale local processing and high solar cell efficiencies in industrial production. Indeed, local laser processing is making its way into industrial production lines today. Laser processing only be successfully understood if the process does not have a negative impact on the quality of the solar cell materials. So as to develop low damage laser processes, essential insight into the physical interaction between the laser and the solar ell materials is definitely crucial. Using pulsed laser sources, the laser-material interaction will depend on laser pulse duration, laser wavelength and material properties. Essential understanding of these dependencies will give understanding of the laser parameters required for successful laser processes. A useful means of understanding exactly what lasers do within solar manufacturing is to categorize the different laser / material interactions (Patrick, 2008). Essential knowledge about laser-material interaction could be useful in the field of silicon photovoltaic (Becquerel, 1839).

Photovoltaic (abbreviated PV) is the most direct way to convert solar radiation into electricity and is based on the photovoltaic effect, which was first observed by Henri Becquerel in 1839 (Becquerel, 1839). Photovoltaic (PV) devices can effectively convert sunlight into clean electrical power and could provide a virtually unlimited amount of energy to our world. Crystalline Si (c-Si) solar cells with thicknesses between 150–300 μm have dominated the market for decades and very high efficiency (~25% at one sun) cells of this material have been realized (Goetzberger, 2005).

Crystalline silicon solar cells operate by absorbing light and using the discrete energy from the received photons to pump electrons to their exited state. The excited electrons migrate through the material's layers and produce an electrical current.

For practical use solar cells are packaged into modules containing either a number of crystalline Si cells connected in series or a layer of thin-film material which is also internally series connected. The module serves two Purposes: It protects the solar cells from the ambient and it delivers a higher voltage than a single cell, which develops only a voltage of less than 1 volt.

The strive towards low cost, high efficiency solar cells has led to the introduction of several new processing tools and techniques that have enabled the impressive cost reductions seen in the PV industry. One group of tools that has the potential to change existing production techniques, and enable new processes and even new solar cell designs are lasers. Surface texturing can be accomplished in a number of ways (Thorstensen ,2013).A single crystalline substrate can be textured by etching along the faces of the crystal planes and the resulting shape of is pyramids like and this is due to crystalline structure of silicon. This type

of texturing is known as "random pyramid" texture, and is commonly used in industry for single crystalline wafers (Brongersma, 2014).

Type of surface texturing known as inverted pyramid texturing, in this type the pyramids are etched down into the silicon surface rather than etched pointing upwards from the surface. For multicrystalline wafers photolithographic technique and mechanically sculpting the front surface using dicing saws or lasers to cut the surface into an appropriate shape are commonly used techniques (Dobrzanski, 2001).

Main objective of this work is the use of surface texturing by means of laser processing and investigation of the influence of laser texturization on the operational properties of the photovoltaic cell in order to enhance the filling factor which leads to efficiency development of the silicon solar cell.

1.2. Literature review:

A. Zoubir *et al* (2002) proved the ability of femtosecond material micro-processing to produce very fine surface structures and its versatility both in the type of processing and the type of materials to be processed. Comparison between the femtosecond and nanosecond regimes has shown one more time that finer, more energy-effective and more material-independent structuring could be obtained with femtosecond pulses (Zoubir, 2002).

Arnaud Zoubir *et al* (2003) characterized dynamics in two types of silicate glasses having different compositions. The differences observed were explained by the self-focusing effect. Examples of device fabrication illustrate the practical use of femtosecond material processing (Zoubir, 2003).

Catalin Florea *et al* (2003) mentioned that both straight and curved waveguides written in a variety of silicate glasses using near-IR femtosecond laser pulses. Writing parameters are identified that produce waveguides that support only a single mode and yield smooth-mode profiles. The laser pulse-induced refractive index change is reconstructed from near-field mode profile data using the scalar wave equation and by refractive near-field profiling. Both coarse and fine period gratings are written and characterized, and the thermal stability of these gratings is investigated. The utility of the femtosecond writing technique is demonstrated by fabricating an optical interleaver (Florea, 2003).

A .Zoubir *et al* (2004) processed buried tubular waveguides having an annular core in bulk PMMA by femtosecond laser direct writing. The refractive index profile was obtained from selective etch profiling. Numerical calculation of the propagating modes in the waveguides was effected with a finite-difference method. Good agreement was found

between calculation and measurement of the output distribution in the near field (Zoubir, 2004).

D.M. Kro *et al* (2004) revised their work on fs-laser fabrication and describing of photonic structures in glass and discuss the effect of glass composition on processing parameters and structural adjusting (Kro, 2004)

Bo Tan *et al* (2005) presented a direct ablation technique for the fabrication of gratings by interfering femtosecond pulses in a specially designed optical configuration. This technique ensures that gratings are formed only at the focal point. The grating line-width can be varied with minor adjustment to the optical configuration. This configuration not only simplifies the optical set-up, but also immunizes the system to extraneous and inherent vibrations, thus enabling gratings of good edge acuity. With this technique, they have successfully fabricated planar gratings of different line-widths on a silicon substrate. This method offers a new approach of the fabrication of a grating on a surface by direct ablation. Also, the feasibility of effectively writing internal gratings in transparent materials are discussed (Tan, 2005).

Kazuyoshi ITOH (2006) studied the refractive index changes and vacancies that are induced in transparent materials like glass by the irradiation of femtosecond laser pulses. He applied this technique to fabricate three-dimensional photonic structures such as optical data storages, waveguides, gratings, and couplers inside a wide variety of transparent materials. He reported micro-fabrication experiments of optical elements in glasses with femtosecond laser pulses, including fabrication of couplers, Bragg gratings, and zone plates and holograms on the surface of glass. A trial fabrication experiment on organic materials is also reported (Krishnan, 2006).

R. Krishnan *et al* (2006) informed the development of high quality dense alumina coatings for providing electrical insulation for DC induction pumps of PFBR. Using of high power lasers to transform the metastable γ-Al_2O_3 phase present in as-deposited Air Plasma Sprayed (APS) alumina coatings into thermodynamically stable α-Al_2O_3 phase is proved. A host of solid-state analytical techniques including non-destructive laser based optical techniques that have the potential for on-line adaptation have been developed in-house (Krishnan, 2006).

Graham D. Marshall *et al* (2006) include optical waveguides that incorporate Bragg gratings written in bulk fused silica by using the femtosecond laser direct-write method and without the need for lithography or ion-beam techniques. A single manufacturing process is used to create waveguide–Bragg grating reflectors for operation in the C band (Grahama, 2006).

Craig B. Arnold & Piqué (2007) proved the range of materials processing capabilities, essential research opportunities, and commercially viable applications that can be achieved using recently developed laser direct-write techniques (Craig, 2007).

L.A. Dobrzański & Drygała (2008) proved the method of texturing of multicrystalline silicon surface using Nd:YAG laser appeared to be much more independent on grains crystallographic orientation compared to conventional texturing methods. Laser texturing makes it possible to increase absorption of the incident solar radiation (Dobrzanski, 2008).

K.C.Vishnubhatla *et al* (2008) fabricated micro gratings in silicate, Foturan ^{TM}, and tellurite glasses using femtosecond direct writing. Refractive index change in these structures was estimated using optical diffraction technique and was found to be in the order of 10^{-3} sufficient for wave guiding applications. The ability to create such structures, both

passive and active, has strong implications in the field of micro-photonic and microfluidic devices (Vishnubhatla, 2008).

M.Taleb *et al* (2011), detected and proved the experimental evidence of the effect of femtosecond laser pulses on the spectral response of a Silicon photovoltaic cell. The observed enhancement is related to the appearing of nano-structured groves in the 700-900 nm range. The responsivity and the conversion efficiency of the photovoltaic cell are enhanced by this technique. Ultra short laser pulses should be still economically reasonable in a large scale production (Taleb, 2011).

J. Thorstensen et al (2011) studied Laser assisted texturing for thin and highly efficient monocrystalline silicon solar cells. A process was developed for production of inverted Pyramids and patch textures on <100> - oriented monocrystalline silicon for light-trapping. These textures have a high potential for light-trapping, but are normally produced by Photolithography. The process described is based on the use of a laser to Create openings through an etch barrier, after which KOH etching of the underlying silicon develops a pattern consisting of <111> crystal orientations. The geometrical accuracy of the laser system is good, and the structures develop as intended, resulting in a texture with up to estimated 94 % area coverage (Thoretensen, 2011).

A. Bauma *et al* (2011) stated on the fabrication of optical Bragg type phase gratings in polymethyl methacrylate substrates by a femtosecond Ti: Sapphire laser. As for their optical characterization, a spatially resolved microscopy interferometry technique is used to detect the two-dimensional distribution of the refractive index change produced by the irradiation process. The results suggest that efficient modification of the material can be accomplished for a regime of repeated pulses with long pulses, 250 fs with low laser fluency (Baum, 2011).

Kais A. Alnaimee in (2011), he used fast laser texturing technique to produce Micro/Nano surface textures in Silicon by means of UV femtosecond laser. He had prepared good absorber surface for photovoltaic cells. The textured Silicon surface absorbs the incident light greater than the non-textured surface. His results show a photovoltaic current increased about 21.3% in two dimensions laser textured area (Alnaimee, 2011).

Luis A. Fernandes *et al* (2011) harnessed femtosecond laser induced birefringence in fused silica waveguides for the first time to demonstrate polarization beam splitting in buried optical circuits. Moderately strong extinction ratio of up to -24 dB was noted for 2 cm long devices. The polarization beam splitters are sufficiently wavelength selective to be attractive for wavelength-division multiplexing (WDM) application and promise to open new directions for creating polarization dependent devices in three dimensional optical circuits, and reported that the means to extend the bandwidth for such polarization splitting will require further design and laser process development (Fernandes, 2011).

J. Thorstensen et al (2012) 2D periodic gratings by laser processing.In this work contribution a process for producing diffractive structures in silicon is presented. The process, a monolayer of polystyrene microspheres is this time applied onto the etch barrier. In the laser processing step, the microspheres act as focusing elements, and serve to increase the spatial resolution of the laser to below 1 μm. An isotropic etch develops a texture consisting of nearly hemispherical dimples in a honeycomb pattern. The process is applicable to monocrystalline silicon with any crystal orientation, or to multicrystalline silicon. With this masked etching process, only the silicon from the dimples is removed, causing a thinning of the silicon wafer of below 350 nm, ideally suited for thin silicon wafers where preservation of wafer thickness is crucial. The

paper serves as a proof of concept of the remarkable increase in spatial resolution brought about by the application of the micro-lens array made up by the microspheres (Thorstensen, 2012).

J. Thorstensen et al (2012) Temperature dependent ablation threshold in silicon using. Ultra-short laser pulses are considered. Experiments are performed showing that the ablation threshold fluence varies with silicon substrate temperature. A numerical model is established, considering the dynamics of the absorption of the incoming laser light, i.e. the energy deposition, and the generation dynamics of conduction band electrons. From this model, information about the dominating physical processes is extracted, and the experimentally observed temperature dependence is reproduced in simulations. The paper contributes to new knowledge on the temperature and wavelength dependence of the ablation threshold of silicon using ultra short laser pulses, in addition to interpretations on the underlying physical mechanisms (Thorstensen, 2013).

D.A. Zuev et al in (2012) they perform experiments on the “black” mc-Si surface fabrication by the nanosecond pulses of the YAG laser second harmonic and on application of the introduced laser texturing method for the mc-Si solar cells efficiency improvement is represented. The developed version of laser texturing permits producing a low-reflection mc-Si surface with the reflectance of ~3% in the spectral range of 0.3-1 μm. The application of the introduced laser texturing method in mc-Si solar cells fabrication makes it possible to increase the short circuit current density and quantum efficiency (Zuev, 2013).

V. Oliveira et al (2012), reported on a simple method to obtain surface gratings using a Michelson interferometer and femtosecond laser radiation .in the optical laser setup used, two parallel laser beams are generated using beam splitter and then focused using the same focusing

lens. An interference pattern is created in the focal plane of the focusing lens, which can be used to pattern the surface of materials. The main advantage of this method is that the optical path difference of the interfering beams is independent of the distance between the beams. The potential of the method was demonstrated by pattering surface grating with different periods on titanium surface in air.(Oliveira, 2012).

Jostein Thorstensen et al (2013), Investigation of depth of laser damage to silicon as function of wavelength and pulse duration. This work describes an experiment determining the depth of laser induced damage Ultra short laser pulses at three wavelengths are applied to silicon Substrate. Thereafter, a controlled wafer thickness is removed by wet chemical etching, and the wafer is passivated. The minority carrier lifetime is measured as function of etch depth and the depth where bulk lifetime is restored gives a measure of the depth of the laser induced damage. The results are compared with previous investigations by Engel hart and show that the depth of damage is severely reduced when going to ultra-short laser pulses, as a result of reduced thermal diffusion and increased optical confinement due to non-linear absorption. While thermal and optical confinement is expected when using ultra short laser pulses, the presented quantitative experimental evidence on silicon is novel [(Thorstensen, 2013).

In addition, an estimate on the minority carrier lifetime in the laser damaged volume is presented. These calculations are also novel in the context of laser damage.

Jostein Thorstensen et al (2013) Laser ablation mechanisms in thin silicon nitride films on a silicon substrate.

In this work the ablation of silicon nitrides with varying index of refraction from silicon is investigated. Varying laser pulse duration and three laser wavelengths are applied, and the mechanism for ablation is

investigated. In this work, TEM analysis was performed by Ragnhild Sæterli (NTNU). A transition region is observed when using a wavelength of 515 nm, where the ablation goes from indirect to direct. In some cases, both direct and indirect ablation is observed in the same spot. In these cases, it is found that the free-carrier contribution must be significant in the interaction between the laser pulse and the dielectric silicon stack. The focus in this article on the underlying physical mechanisms of silicon nitride ablation is novel (Thorstensen, 2013).

Jostein Thorsten et al (2013) “New approach for the ablation of dielectrics from silicon using long wavelength la contribution shows a different approach to ablation of dielectrics from semiconductors. By investigating the absorption characteristics of silicon and various PV-relevant dielectrics, it is found that in the mid- to far-IR; silicon is transparent, while the dielectrics are absorbing. This behavior is interesting, as it opens for energy deposition in the dielectric rather than in the silicon, potentially resulting in lower substrate damage. For the measurements of absorption in dielectrics, Ørnulf Nordseth (IFE) prepared samples with aluminum oxide (AlOx), and Halvard Haug (IFE) prepared samples with silicon dioxide. Simulations on the temperature dynamics of the process are performed, and it is seen that short laser pulses may be able to remove the dielectric without melting the silicon substrate. In experiments however, signs of melting of the silicon are found, indicating that pulse duration of 100 ns is still too long. As such, the paper brings the idea of a new process, while it remains to be proven if the process can be successful using shorter laser pulses (Thorstensen, 2013).

Kallepalli Lakshmi Narayana .Deepak *et al* (2013) stated that spectroscopic properties of fs laser irradiated polymers and LNB crystal. In case of polymers observed emission from the fs laser modified regions

and it is found to be shifting with the excitation wavelength due to various transitions involved in functional groups and red edge effect. Also these materials exhibited paramagnetic upon fs laser irradiation unlike LNB crystal. Confocal micro Raman studies revealed broadening in case of polymers which is an indication of the presence of radicals and or defects which are confirmed through emission and ESR studies. Fs laser irradiated LNB crystal also showed the presence of defects but they do not exhibit the properties of emission and paramagnetic (like polymer media) due to absence of functional groups (Kallepalli, 2013).

J. Thorstensen et al (2013) Light-trapping Properties of a Diffractive Honeycomb Structure in Silicon In this paper, the honeycomb structure generated. Firstly, the texture is applied to large area, by utilizing a top-hat beam shaper, an optical component transforming a Gaussian beam profile to a uniform, square intensity distribution. The structure is applied to silicon wafers with a thickness of 21 – 115 µm. Optical absorption characteristics were measured by Jo Gjessing, who also analyzed the contributions to optical loss. The observed trends are explained and the diffractive honeycomb textures are compared with random pyramids, isotropic etched samples and polished wafers, as these constitute various relevant references. It is found that the diffractive honeycomb structure delivers light trapping that surpasses many of the relevant references showing a photogenerated current of 38 mA/cm^2 on 21 µm thick wafers. As such, the texture has the potential to provide a significant increase in on wafers where random pyramids cannot be efficiently applied, e.g. for kerf-less wafers with a non-<100> crystal orientation (Thorstensen, 2013).

J. Thorstensen et al (2013) Light-trapping properties of Patch textures created using Laser Assisted Texturing. In this paper, the light-trapping properties of the patch texture developed were of great

assistance during the optical measurements. Optical absorption measurements on a patch textured silicon wafer are performed and these zeasurements are compared with ray-tracing simulations. This enables us to extract information about the quality of the texture. From these simulations, the current-enerating potential of the textures is extracted. It is found that the created texture gives an increase in of up to 0.5 mA/cm^2 compared to the random pyramids texture, and as such, it is concluded that it is possible to generate high quality textures with laser based methods. The process would be interesting for application on <100>-oriented monocrystallin Silicon. It is recognized that the process must be simplified in order to justify the added Process complexity (Thorstensen, 2013).

Ali A. S. Marouf *et al* (2014) utilized a fast laser texturing technique to produce micro/Nano surface textures in Silicon by means of UV femtosecond laser pulses. They showed and investigated the experimental evidence of the effect of femtosecond laser pulses on the spectral response of a Silicon photovoltaic cell, and found that the use of this method leads to improve the responsively and the conversion efficiency of the photovoltaic cell. The irradiation process leads to the formation of Micro- Nano meter periodic structure on substrates with a large area using single or double exposition. This technique is much cheaper and simpler than the electron beam lithography (Marouf, 2014).

1.3 Problem Statement

The high cost in production of electricity from solar cell due to manufacturing of this device and due to their low efficiency, the efficiency of solar cells is about (24%) in Lab, and only of about (13%) in the use per cell (Thorstensen, 2013).

Laser surface applications shows great opportunity to enhance the solar cell efficiency via surface texturing in order to reduce both reflection and recombination losses and increase the absorption , hence improvement of solar cell efficiency.

1.4. Objectives

This work aimed mainly to:

- Formatting the photovoltaic solar cell (PV) samples with requested area by searching and taking measurements fill factor (ff) and efficiency before the irradiation process.
- The photovoltaic solar cell (samples) irradiation (surface texturing) by using co_2 laser for two dimension areas (1cm × 1cm, 2cm × 2cm and 3cm × 3cm).
- Testing the performance of the photovoltaic solar cell after the irradiation process through the calculate of filing factor (ff) and efficiency.
- Study the surface morphology of the textured photovoltaic solar cell using scanning Electron microscope (SEM).

1.5 Thesis formatting

The thesis comprises of four chapters; chapter one contains a short introduction, Problem statement, study objectives and Literature review were given in this chapter. Chapter two involves detailed theoretical background cell efficiency, silicon solar cell materials and technology,

Laser Material processing in crystalline silicon photovoltaic and chapter three cover the experimental part of this study, a setup used to study the IV curve of the solar cells and each component with it is specifications. Finally chapter four includes the results and discussion of this study, the surface morphology photovoltaic solar cell using scanning Electron microscope (SEM) was study and conclusion, recommendations for future works and list references of will be presented in the end of this chapter.

Chapter Two

Theoretical Background

2.1 Historical development of cell efficiency

In 1941 the first silicon solar cell was reported by Ohl *et al.* (Helmreich, 1981), It featured a melt-grown pn- junction and an energy conversion efficiency of less than 1%. A large progress was then achieved in the early 1950ies where Pearson, Fuller and Chapin in the Bell Laboratories prepared silicon solar cells with a diffused pn-junction. The first cells were fabricated on p-type silicon and reached efficiency up to around 4.5% (Staebier, 1977), and then they switched to arsenic-doped n-type silicon with a boron-doped emitter (Erge, 2001), this increased efficiency to a value of more than 6%. The first application for these "solar batteries" was the power supply of satellites. It won the competition against other power supplies as chemical batteries (Becker, 1997), the space race was of national interest for Americans and Soviets during the cold war and solar cells played an important technical role. In fact, today photovoltaic panels are still the dominant power source for satellites and other space applications. Up to the end of the 1950s the cells were mainly fabricated on n-type silicon leading to superior efficiencies up to around 14%. However it was found that space radiation hardness was less detrimental for cells with a p-type base (Gamberale, 2002), This was getting even clearer when a high-atmosphere nuclear bomb was ignited by the Americans leading to failure of the solar panels of satellites [Wilk, 2001], Thus in the early 60ties there was a switch to cells on p-type silicon with a phosphorus-doped emitter, These cells had a higher radiation hardness but started with a lower efficiency. It took up to 1973 to achieve higher efficiencies with cells on p-type silicon than those reached in the early 1960ies with cells on n-type base.

A second strong phase of cell development started in 1980s with the passivated emitter solar cell (PESC) clearing the important 20%-hurdle in 1985 (Kaltschmitt, 1993), The PESC[1] cell and also its successors the PERC[2] (Nitsch, 1993) and the PERL[3] (Goetzberger, 1998|) solar cell have a very important feature in common: surface passivation in order to reduce recombination of charge carriers at the surfaces. Indeed this is a crucial prerequisite for all high-efficiency silicon solar cells particularly for interdigitated back-contact cells (Goetzberger, 1998, Palm, 2000) where the collecting junction is at the rear side and most carriers have to diffuse a long way. Back-contact cells played always an important role in the race for record efficiencies and are the base structure for today's best commercial solar cells with efficiencies greater than 22%. The best efficiency for a monocrystalline silicon solar cell is 25% (Staebier, 1977-Dietl, 1981) getting quite close to the "practical" limit of around 26% (Goetzberger, 1997), although cell efficiencies on monocrystalline silicon are significantly higher, it is very important to keep an eye on cells on multicrystalline silicon since 5 out of 10 solar cells today are made of this material type. Multicrystalline silicon is cheaper than monocrystalline silicon but unfortunately has also a lower material quality due to a higher amount of crystal defects and metal impurities. Since this difference in material quality is especially relevant for record solar cells where hyper-pure floating-zone (FZ) silicon is used for mono cells, it is fair to report record efficiencies for multi cells separately. The major interest in multicrystalline silicon started mid of the 70ies with record efficiencies around 15%. In this case the historical increase in efficiency was mainly influenced by improving the material quality either during the crystallisation process or the cell process utilizing gettering and internal hydrogen passivation of crystal defects. An effective way to reduce the influence of material quality is the reduction of cell thickness and usage

of effective surface passivation. This path led to today's record solar cell on multicrystalline silicon with an efficiency of 20.4% and a thickness of only 99 pm (Goetzberger, 1997) (Block, 2000),

1. PESC = Passivated Emitter Solar Cell
2. PERC = Passivated Emitter and Rear Cell
3. PERL = Passivated Emitter, Rear Locally diffused cell

2.2 Maximum Achievable Efficiency

Talking about efficiencies of solar cells a major question is of course: How far can we get? the answer to this question was given in a very elegant way by Shockley and Queisser already in the 1960s (Nussbaumer, 1996), Based on a detailed balance calculation for the ideal case that the only recombination channel is radioactive recombination, they calculated the maximum achievable efficiency which is around 30% for band gap of 1.1 eV (sic!).

Fig. 2.1 visualizes the main loss mechanism in a silicon solar cell: spectral losses. It shows the maximum achievable energy of a silicon solar cell in relation to the sun spectrum. Photons carrying a specific energy can only generate one electron-hole pair even if their energy is higher. The excess energy greater than band gap energy is lost in thermalization of the hot carriers i.e. heat (see upper grey part in Fig. 2.1). Photons with energies lower than the band gap cannot generate an electron-hole pair (non-absorption, right grey part in Fig. 2.1). These two losses account for about 50% of the power carried in the sun spectrum.

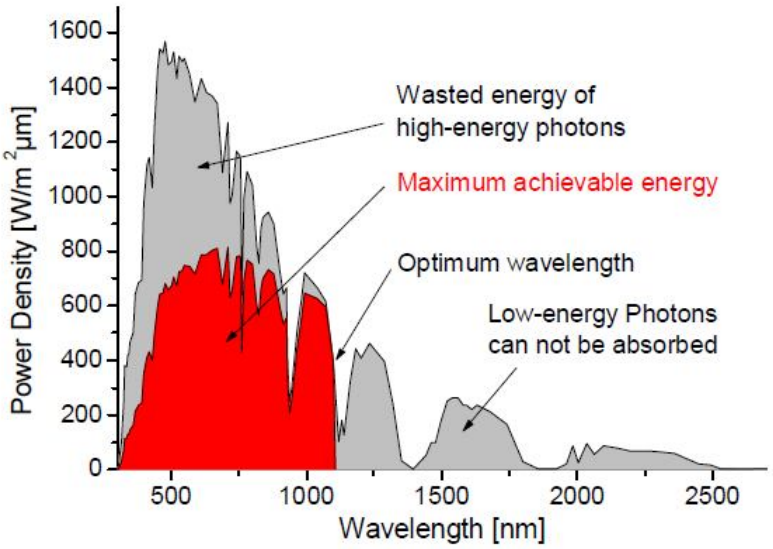

Fig. 2.1 Spectral losses in a solar cell the figure show the maximum achievable energy of a silicon solar cell in relation to the sun spectrum (AM1.5).

In contrast to the calculation of Shockley and Queisser, in a realistic crystalline silicon solar cell radiative recombination does not play a dominant role due the indirect band structure of silicon. Instead of this Auger recombination is dominating. Recent accurate determination of the Auger coefficients in silicon have led to calculation of the maximum achievable efficiency for a silicon solar cell being 29% (Ciszek, 1984), however such an idealized device without contacts is only of interest in theory and cannot be realized. For realistic but optimized silicon solar cell an efficiency limit of 26% was predicted (Goetberger, 1997).

2.3 Silicon Solar Cell Materials and Technology

2.3.1 Silicon Material

Apart from oxygen, silicon is the most abundant element in the surface of the earth. It almost always occurs in oxidized form as silicon dioxide, as in quartz or sand. In the refining process, SiO_2 is heated to about 1800◦C together with carbon. The metallurgic grade silicon that results from this process is used in large quantities in the iron and aluminum industries. Since it is only about 98% pure, it is not suitable as a semiconductor material and has to be further refined. This is done by transferring it into trichlorosilane ($SiHC_{13}$), which is a volatile liquid. This liquid is distilled and subsequently reduced by reacting it with a hot surface of silicon, the Siemens process. Those two processes require a considerable input of energy and are the major contribution to the energy content of silicon solar cells (Green, 1999).

2.3.2. Mon crystalline and Multicrystalline Silicon

In the beginning, only Czochralski (CZ) grown single crystals were used for solar cells. This material still plays an important role. Figure 2.2 shows the principle of this growth technique. Polycrystalline material in the form of fragments obtained from highly purified polysilicon is placed in a quartz crucible that itself is located in a graphite crucible and melted under inert gases by induction heating. A seed crystal is immersed and slowly withdrawn under rotation. At each dipping of the seed crystal into the melt, dislocations are generated in the seed crystal even if it was dislocation free before. To obtain a dislocation-free state, a slim crystal neck of about 3mm in diameter must be grown with a growth velocity of several millimeters per minute. The dislocation Free State is rather stable, and large crystal diameters can be grown despite the high cooling strains in large crystals.

Today, crystals with diameters of 30 cm and more are grown routinely for the semiconductor market. For solar cells smaller diameter crystals are grown because the usual solar cell dimensions are 10 cm by 10 cm or sometimes 15 cm

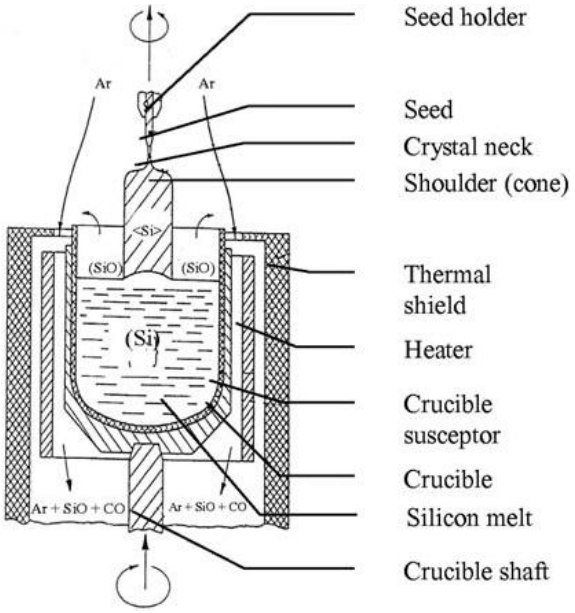

Fig. 2.2. Principle of the Czochralski growth technique

By15cm. The round crystals are usually shaped into squares with rounded corners in order to obtain a better usage of the module area.

The silicon melt reacts with every material to a large extent. Only silica can be used as a crucible material, because its product of reaction, silicon monoxide, evaporates easily from the melt. Nevertheless, Czochralski-grown crystals contain 10^{17}–10^{18} cm^{-3} of mainly interstitial oxygen. An alternative crystal growth technique is the float zone technique (Fig. 2.3). A rod of solid highly purified but polycrystalline silicon is melted by induction heating and a single crystal is pulled from this molten zone. This material is of exceptional purity, because no crucible is needed, but it is more costly than Czochralski (Cz) material. In particular, it has a very low oxygen contamination which cannot be avoided with the Cz material because of the quartz crucible. Float zone (Fz) material is

frequently used in R&D work. Record efficiency solar cells have been manufactured with float zone material, but it is too expensive for regular solar cell production, where cost is of overriding importance.

An interesting new development concerns tricrystals (Palm, 2000). These are round crystals consisting of three single crystals arranged like pieces of a pie. They can be grown much faster and have higher mechanical stability. Solar cells of 0.1mm thickness can be manufactured with a saving of 40% of the material.

For solar cells, as well as for all other devices, the crystal rods are separated into wafers of 0.2mm to 0.5mm thickness by sawing. This is a costly process because silicon is a very hard material that can only be cut with diamond-coated sawing blades. The standard process was the ID (inner diameter) saw, where diamond particles are imbedded around a hole in the saw Blade.

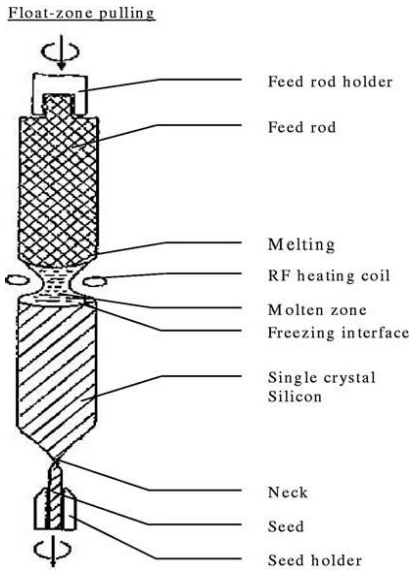

Fig. 2.3. Principle of the float zone technique

A disadvantage of this process is that up to 50% of the material is lost in the sawing process. A new process was developed especially for solar cell wafers, the multi-wire saw (Fig. 2.4). A wire of several kilometers in length is moved across the crystal and wetted by an abrasive suspension

whilst being wound from one coil to another. In this manner, thinner wafers can be produced and sawing losses are reduced by about 30%. It is interesting to note that wire saws are now also used for other silicon devices, an example of synergy in this field.

Another technology dating back to the 1970s is block casting (Dietl, 1981), which avoids the costly pulling process. Silicon is melted and poured into a square graphite crucible (Fig. 2.5). Controlled cooling produces polycrystalline silicon block with a large crystal grain structure. The grain size is some millimeters to centimeters and the silicon blocks are sawn into wafers by wire sawing, as previously mentioned. Cast silicon, also called polycrystalline silicon, is only used for solar cells and not for any other semiconductor devices. It is cheaper than single crystal material, but yields solar cells with a somewhat lower efficiency. An advantage is that the blocks easily can be manufactured into square solar cells in contrast to pulled crystals, which are round.

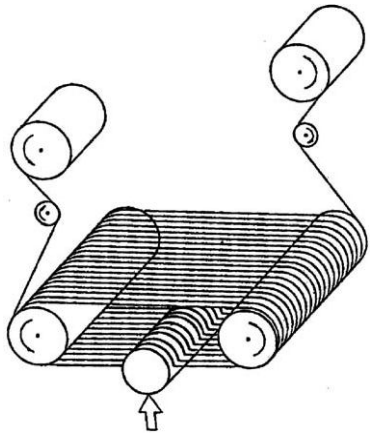

Fig. 2.4. Multi-wire sawing process

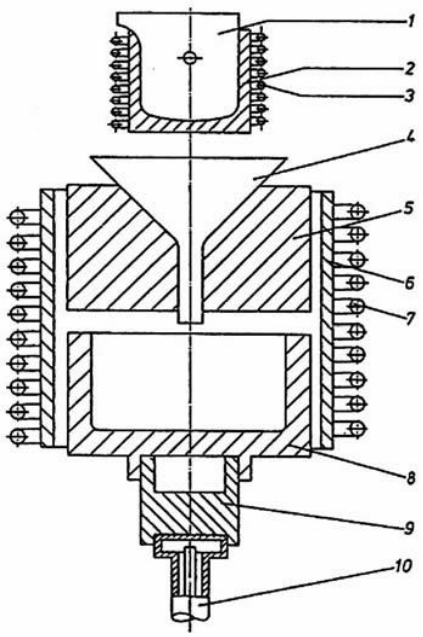

Fig. 2.5. Block casting apparatus

It is much easier to assemble multicrystalline wafers into modules with nearly complete utilization of the module area, thus, the lower efficiency of cast material tends to disappear at the module level. Because of the contact with the crucible, polycrystalline silicon has a higher impurity content and thus lower carrier lifetime and lower efficiency than monocrystalline silicon. Point defects and grain boundaries act in the same direction. Several techniques have been devised to remove impurities during solar cell processing. Mobile impurities can be pulled to the surface by phosphorus gettering (Goetzberger, 1960), which occurs during emitter diffusion. Immobile point defects are deactivated by hydrogen passivation. Atomic hydrogen can diffuse into silicon even at relatively low temperatures. Processed wafers are exposed to atomic hydrogen produced in a plasma discharge.

2.4 Silicon Cell Technology

Cell technology converts the silicon wafers into solar cells. As a rule, p-type silicon is used in the photovoltaic industry. For wafer processing, the following steps are important.

2.4.1 Production of pn and pp+ Junctions

The active junction (emitter) is very close to the front surface. At the rear of the device a high p-doping is introduced to reduce contact resistance and Surface recombination: These junctions are realized by thermal diffusion. In the diffusion process, an electrically heated tube furnace with a quartz tube is used. Diffusion temperatures vary between 800◦C and 1200◦C. All high temperature steps require very clean conditions in order to avoid contaminants. Diffusion sources are phosphorus for the emitter junction and boron for the so-called back surface field, which repels carriers from the high recombination back contact. The doping elements are introduced as liquid or gaseous compounds, e.g., phosphine (PH) or phosphorus oxychloride (POC_{13}) for n-doping, and boron bromide (BBr_3) for p-doping. In industry the back contact is often generated by sintering the aluminum contact. Since Al is a group III element, it will also generate p-type doping. This procedure, however, cannot be used for very high-efficiency solar cells.

2.4.2 Oxidation Process

Oxidation of the silicon surfaces is an important step in solar cell manufacture. It is carried out in quartz tube furnaces like the diffusion process. The oxidation atmosphere can either be dry oxygen or wet, which means oxygen plus water vapor. SiO_2 surface layers have several functions. They passivate the surface by reducing surface states that act as recombination centers. They act as diffusion barriers in selected locations, and they provide mechanical and chemical protection of the sensitive surface against further processing and module manufacturing.

On air they also provide some antireflection property, but in encapsulated cells other materials with higher index of refraction have to be used. Excellent passivation properties can also be obtained with plasma-deposited silicon nitride.

2.4.3 Electrical Contacts

In the laboratory, electrical contacts are mainly made by vacuum evaporation, which is a very controllable technique. In industry, screen printing of thick films, which is more amenable to automation, is used. For the front contacts a paste consisting of 70% Ag, an organic binder, and sintered glass is applied. After deposition, the layer is sintered at approximately 600◦C and a good electrical contact results. Screen printing has several disadvantages. Its lateral resolution is limited, and it only makes good contact to highly doped surfaces. For the back contact, a paste containing aluminum is also screen printed over the entire surface and then sintered. These and other simplifications explain why industrial solar cells have significantly lower efficiency but also lower cost than the best laboratory cells.

2.4.4 Antireflection Technologies

Two measures, which can be combined, are instrumental in reducing surface reflection. The first is surface texturing, which bends incoming rays into a more horizontal direction and thus increases its path length inside the silicon. Surface texturing works only on monocrystalline silicon of _100_ orientation. For texturing, the silicon wafers are immersed in a weak solution of KOH or NaOH at 70◦C. In this way the _111_ orientations are exposed as random pyramids Fig (2.6). Chemical texturing cannot be applied to cast multicrystalline silicon because it consists of crystal grains of different orientations.

The other possibility is to deposit a transparent antireflection layer. For this purpose, a material has to be used for which the refractive index is

$n = (_{n\text{si}}\, _{n\text{s}})^{1/2}$, where n_s is the refractive index of the surrounding medium. Since in industrial production the cells are embedded into modules with a glass cover, its index has to be used. A practically applied material is titanium dioxide (TiO_2). It can also be incorporated into a screen printing paste and treated as described before. An antireflection film can also be combined with surface texturing for high efficiency

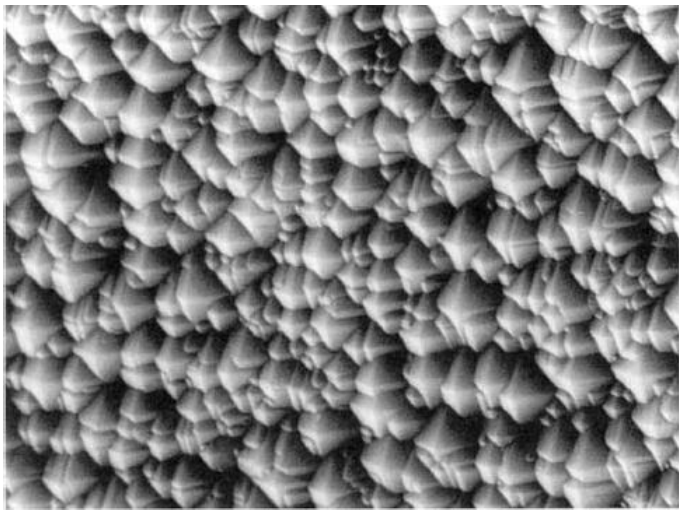

Fig. 2.6. Electron microscopic picture of silicon wafer with random pyramids

2.5 Advanced Si-Solar Cells

2.5.1 High Efficiency Cells

A real solar cell has a number of loss mechanisms, all of which can be minimized. The record efficiencies that have been achieved in the past have been accomplished mainly by careful attention to loss mechanisms. A survey of loss mechanisms can be seen in Fig. 2.7. Optical losses arise from reflection losses at the semiconductor surface. These can be reduced by antireflection

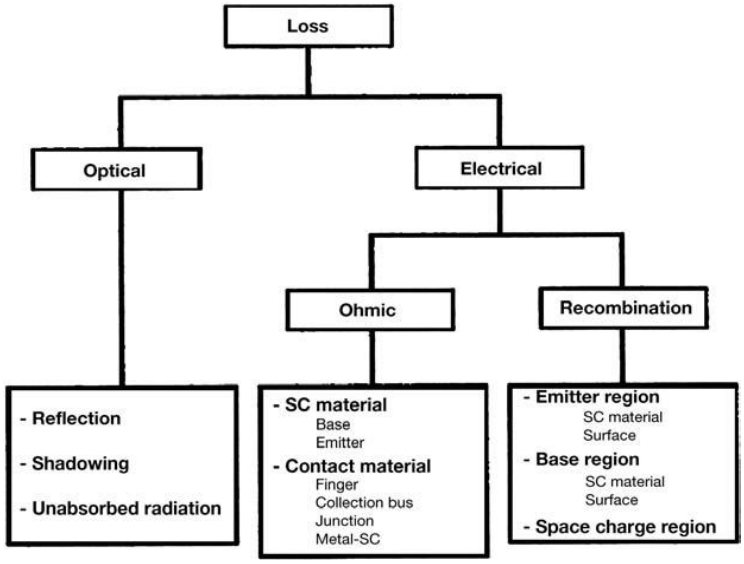

Fig. 2.7 Survey of loss mechanisms in solar cells (SC is solar cell)

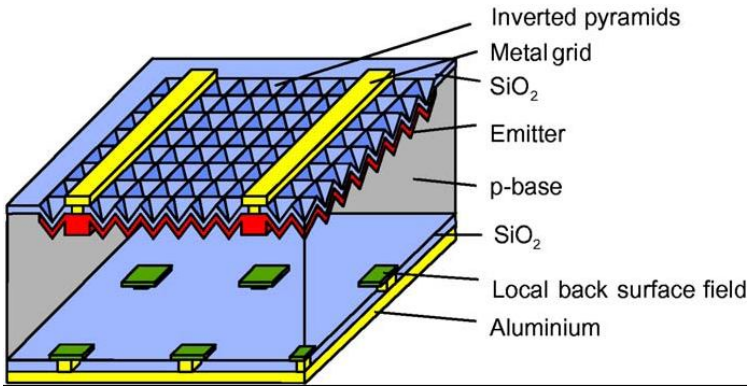

Fig.2.8. Structure of a high efficiency monocrystalline solar cell

Coatings and surface texturing, the electrical losses can be subdivided into ohmic and recombination losses. The ohmic losses arise in the semiconductor material, particularly in the thin emitter layer. In order to reduce these losses, the emitter is covered by a grid of metal fingers, which also contribute to losses. The junction between metal contacts and the semiconductor both at the front and rear can represent a contact resistance, particularly if the contact is to a region of lower doping. These losses can be reduced by locally restricted highly doped regions below the contacts. Recombination losses occur because photogenerated minority carriers can recombine before reaching the pn-junction and thus are lost for current flow. All three regions of a solar cell – the emitter layer, the base, and the space charge region between emitter and base – contribute to recombination and have to design accordingly.

Optimal design principles are incorporated in modern high efficiency cells like the LBSF (local back surface field) (Knobloch, 1994) cell shown in Fig. 2.8. The following details are important for the very good efficiency of the cell, which is of the order of 23%–24%:

– 200-μm-thick base layer of float zone silicon.

– Textured front side with inverted pyramids and antireflection coating to reduce reflection.

– Narrow metal contacts from fingers to local highly doped emitter regions. In this way, recombination losses at the emitter surface are minimized. For good surface passivation, low doping at the surface is required. On the other hand, good ohmic contact can only be made to highly doped regions that also cause high surface recombination velocity. This leads to very restricted, locally doped contact regions.

– The base contacts at the lower side are also restricted for the same reason.

– Good surface passivation.

– The back surface contact has reflective properties and reflects light that penetrates to the back of the cell.

2.5.2 Bifacial Solar Cells

If the thickness of a solar cell is of the order of the diffusion length or smaller, then carriers generated throughout the entire base volume can be collected and the device is light sensitive on both sides. The only change that has to be made is that the rear of the cell has to be open to the light by applying grid fingers similar to the front side. The module also has to have a glass cover on both sides. Such cells are available on the market today. They still have a somewhat lower efficiency on the rear side, but this could be remedied by better design. Laboratory cells have exhibited efficiencies above 20% on both sides.

Bifacial modules can have interesting applications. They can collect light on both sides and in a number of such applications, have higher combined yield than one-sided modules.

2.5.3 Buried Contact Cells

Another type of high efficiency solar cell is the buried contact Si solar cell shown in Fig. 2.9. This structure was first realized in 1985 by M. Green (Hemreich, 1981) and is patented in many countries. The significant difference in this cell is the buried contact. Using laser technology grooves of approximately 20 μm wide and up to 100 μm deep to hold the grid fingers are cut in Si wafers textured according to the principle of random pyramids. The etching process that follows removes the silicon destroyed by this process. These grooves provide two advantages. Firstly, shadowing is reduced significantly when compared with the normal grid structure of commercial solar cells. Values of only 3% surface shadowing are obtained. Secondly, the grooves can be filled with contact metal. Thus, approximately the height of the grooves and thus the metallization can be five times its width. In conventional cells,

even for vacuum evaporated contacts and contacts reinforced by electrodepositing, the ratio

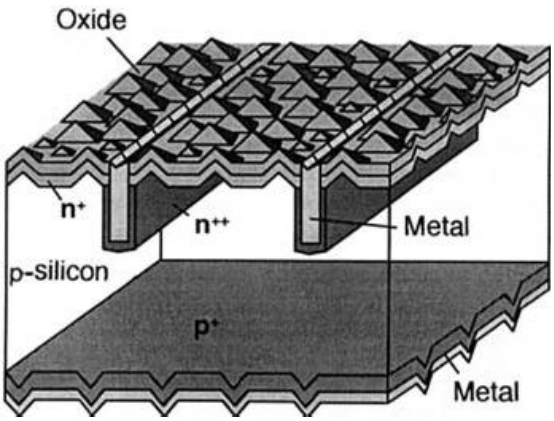

Fig. 2.9. The buried contact solar cell

Is 1: 1, i.e., the metal contact height is equal to its width. The five-fold height means a reduction in the resistance of the contact finger by a factor of 5, resulting in a significantly better fill factor. The technology of metalizing consists of an electro less-deposited nickel contact, which is sintered and then reinforced with copper. Since this technique does not require photo mask processes or high-vacuum evaporation technologies, and is thus significantly more economic, it is well suited for use in serial production. The double-stage emitter is used for the emitter structure, whereby the highly doped n++ film is restricted to the grooves. The p+ back surface field permits higher efficiencies.

A further advantage of this cell is the textured back surface, which increases the confinement of light and thus the total efficiency. With this type of cell (large area), average efficiencies of 18% have been achieved in production. With specific techniques, such as an improved antireflection coating and a local back surface field, efficiencies of up to 21% have been achieved in the laboratory (Wenham, 1994).

2.5.4 Interdigitated Back Contact Cells

The IBC (Interdigitated Back Contact) structure suggested by Lammert etal. (Laramert, 1977) In 1974 was realized by Swanson et al. (Swanson, 1984) and Sinton et al. (Sinton, 1986). As the name suggests, n+ and p+ contacts (Fig. 2.10) lie on the back of the cell. This structure has the following advantages.

– There is no shadowing of light by the finger structure.

– The metal contacts can be broad and take up almost the entire back surface.

They are therefore of very low impedance, thus achieving a very low series resistance. Therefore, these cells are preferably applied in systems with light concentration.

– The penetration depth of n+− and p+− layers are noncritical.

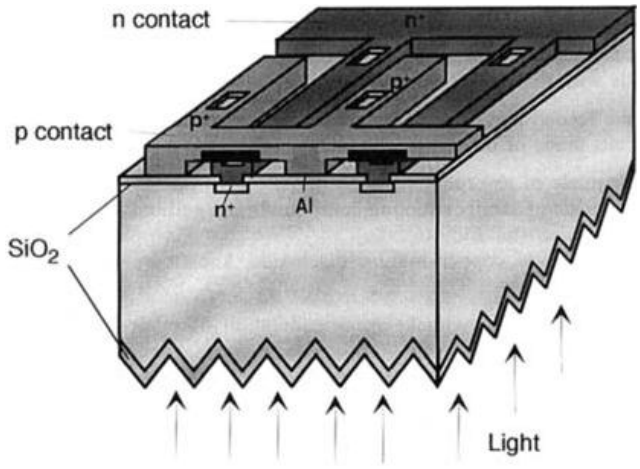

Fig. 2.10. The buried contact solar cell

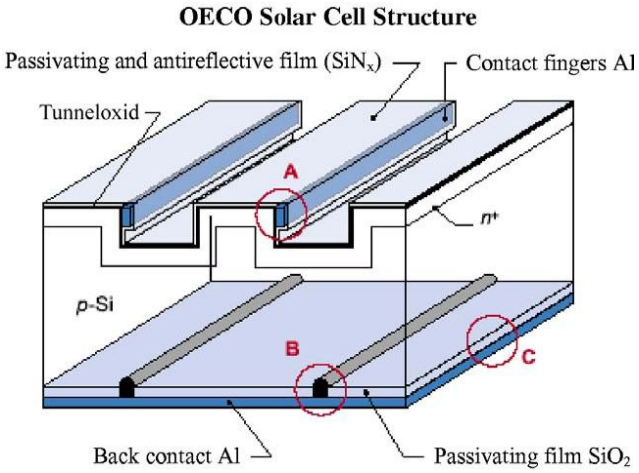

Fig. 2.11.The OECO (Obliquely Evaporated Contact) cell

This concept was further developed into the point contact solar cell in which only localized contacts in small points are made to the base layer. It requires very high quality silicon material and very good surface passivation. So far, it was only made for special applications where efficiency was of more importance than cost, but a simplified version of this cell is now being commercialized by the Sun Power Corporation for the general market.

2.5.5 OECO Cell

The OECO (Obliquely Evaporated Contacts) cell was developed by R. Hezel at the ISFH in Hameln (Hezel, 2002). This is a high efficiency cell that was specifically designed for easy manufacturability. Its basic features are shown in Fig. 2.10. The cell surface has mechanically machined grooves. The Al contacts are at the sides of the grooves such as to avoid light losses by shadowing. Evaporation of contacts is done by arranging large numbers of cells surrounding the evaporation source.

The latest results of this cell are: efficiencies of 20.0% for a 96 cm^2 cell with float zone silicon and 19.4% with czochralski silicon. This type of cell has also been realized as a bifacial cell.

2.5.6 a-Si/c-Si Heterostructures

A very interesting new development is the combination of crystalline and amorphous technologies in heterostructures. Absorption of sunlight still occurs mainly in a wafer of mono- or polycrystalline silicon. The silicon wafer is contacted on both sides with amorphous silicon films. The principle is shown in Fig. 2.12. This technique represents a combination of c-Si and a-Si technologies. This configuration has the following advantages:

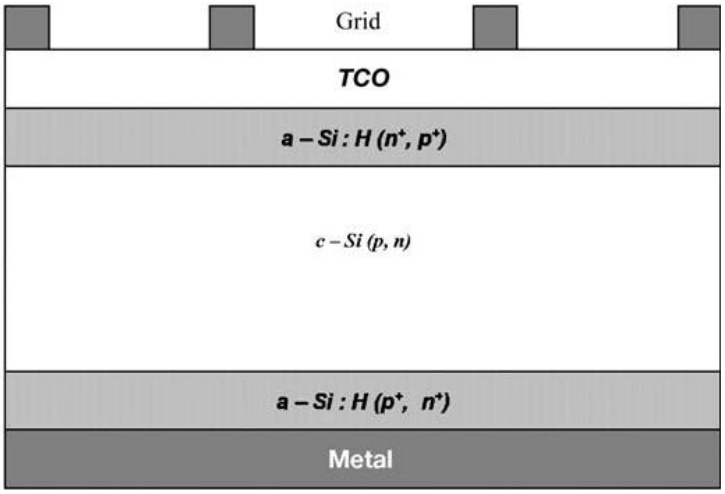

Fig. 2.12. Cross section of a Si/C-Si/a-Si heterostructure

–Potential for high efficiency.

– Very good surface passivation → low surface recombination velocity.

– Low processing temperatures → all processing steps occur below 200◦C.

– Low thermal budget for processing → reduction of energy payback time.

– Reduced cost of cell technology.

The best results with this approach were obtained by the Japanese company Sanyo. The latest achievement is a conversion efficiency of

20.7% for a cell area of 101 cm^2 using n-type CZ-Silicon as the base (light absorbing) part (Sakata, 2000).

Sanyo has developed the HIT-structure (Heterojunction with Intrinsic Thin layer). Its composition is a-Si (p+)/a-Si (i)/c-Si (n)/a-Si (i)/a-Si (n+). Very crucial in this structure is a thin intrinsic a-Si layer contacting the c-Si on both surfaces. This is apparently important for achieving good surface passivation. Interesting is that the crystalline silicon is n-type material. Because of the low conductivity of a-Si, a front window layer of a transparent conductor is required.

According to the information provided by Sanyo, the solar cells have excellent stability. Sanyo is now marketing this new type of cell.

2.5.7 Rear Side Contacted Cells

Recent developments in silicon solar cell technology exploit the advantages of thin wafers. Thinner wafers have economic and physical advantages. The most important effect of using thinner wafers is that the amount of expensive silicon material per cell is reduced. From the view point of device physics, it can be shown that thin wafers can lead to higher efficiency, provided recombination at the back contact can be minimized.

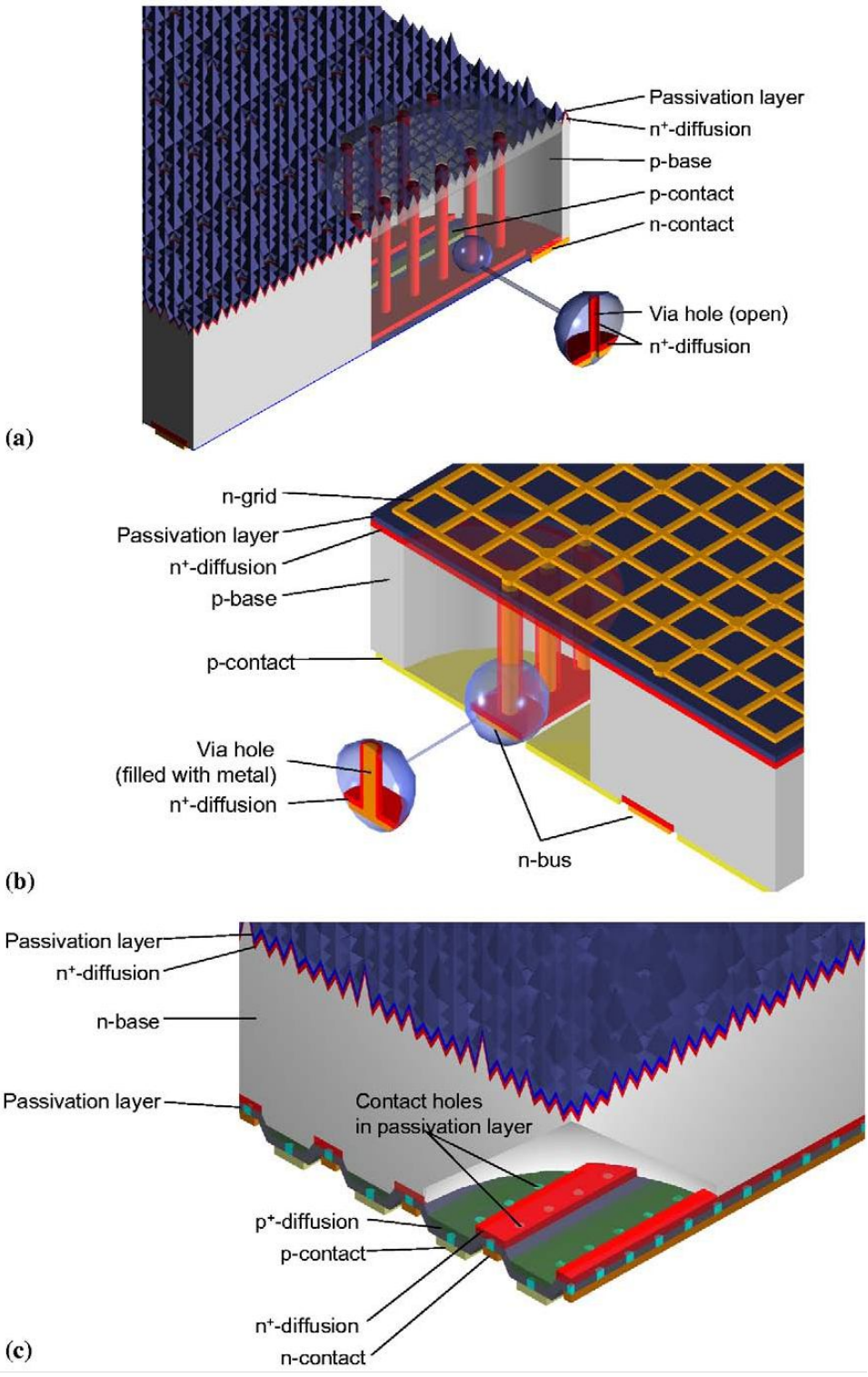

Fig. 2.13. (a) The emitter wrap through cell, (b) the metal wrap through cell, (c) the point contact solar cell

Thin silicon wafers permit new technologies for the contacts. Both n and p-type contacts can now be moved to the rear side. There are three different technological solutions for this task (Fig. 2.13a–c):

– The point contact cell which is an improved version of the interdigitated back contact cell shown in Fig. 2.10.

– Emitter wrap through cell (Gee, 1993).

– Emitter contact wrap through cell (Kerschver, 1998).

The last two types are made by laser drilling holes through the silicon. In the emitter wrap through cell, the n-type emitter is brought to the rear side of the cell and both emitter and base contacts are made there in interdigitated manner. The emitter diffusion also covers most of the rear of the cell. The emitter metal contact cell is similar, with the difference that the emitter metal contact fingers are still at the front side but connected through metal filled holes to the rear. The difference of this technique is that fewer holes are required.

Such cells have the following advantages:

– Little or no shadowing of the front by metal grids, therefore, more light current.

– The front of the cells and modules has a very uniform appearance, an important aspect for architectural applications.

– Series connection of the cells in the modules is much simpler, because all connections are in the same plane.

– Lower quality silicon material can be employed, because the emitter junction is on both sides of the cell and, therefore, carriers have to diffuse not more than half the cell thickness.

2.5.8 Laser-Fired Contact Cells

Laser-Fired Contact (LFC) cells (Fig. 2.14) offer the possibility for mass production of high efficiency solar cells like the LBSF with local back surface field (see Fig. 2.9). The localized back contacts involve expensive

photolithography steps and so are not attractive for production. The new technology avoids this step by rapid laser firing of the contacts. The rear side of the cell is first

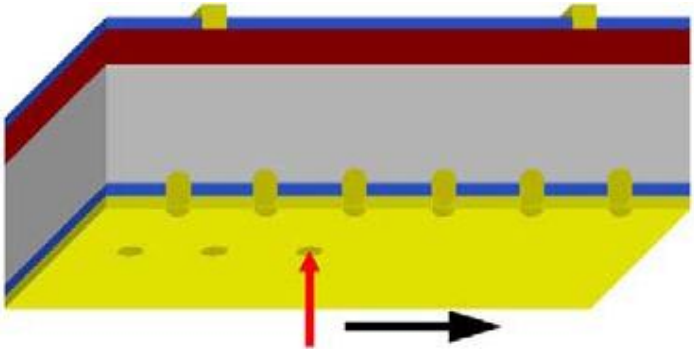

Fig. 2.14. The laser (vertical arrow) is scanned across the rear side of the cell, forming localized contacts

Passivated by silicon nitride film and then an aluminum layer are applied. Then, the local contacts are produced by scanning a q switched Nd-Yag laser across the wafer. An entire 10 cm by 10 cm wafer can be processed in about 2 sec. The contacts are at 1mm centers. The laboratory results are excellent: Efficiencies up to 21.3% have been reached (Schneiderlochner, 2002).

Advantages of LFC cells:

– No warping of wafers compared to complete Al-covered rear sides, very important for thin wafer processing.

– Very good light reflection at the rear side.

– The laser-fired contacts form functional back contact fields.

Very high efficiencies comparable to much more complex cells have been achieved.

2.6 Laser Material Processing in Crystalline Silicon Photovoltaic

Lasers play a major part in the processing of the numerous materials used in engineering and manufacturing, the range of processes in which lasers are involved is over increasing. One of the areas in which laser has recently found application in energy system, which the dwindling non-renewable sources of energy such fossil and increasing demand of electricity, there is increasing interest in addressing the energy problem through development of systems for renewable energy alternatives such as solar energy. Though solar energy is readily available and has no adverse effects on environment such as pollution and greenhouse effects, it has not been fully exploited due to a number of challenges. Some of these challenges include high capital cost and the low conversion efficiency. Therefore photovoltaic industry has taken advantage of the benefits inherent in laser technology, namely accuracy, cost-efficiency, and flexibility that are critical in manufacturing today (Alphonse, 2012).

2.6.1 Introduction to Laser Materials Processing

OVER the last two decades laser processing has become an indispensable part of competitive manufacturing throughout the world. Whether the project involves metal, glass, plastic, silicon, rubber, or even wood, laser materials processing has proven its superiority in terms of accuracy and process efficiency. The term “laser materials processing” refers to a number of different types of processes all utilizing the unique benefits offered by laser light. These processes include welding, cutting, cladding, heat treating, machining and drilling which are easily accomplished with lasers instead of traditional manufacturing techniques, tools and machinery.

Laser processing has a number of important benefits over other available methods. One of the benefits of laser processing is its ability to work with many different types and shapes of materials. Traditional drilling methods, for example, are difficult to use on rounded materials. With laser drilling, a non-contact process, geometric limitations are easily overcome with conventional or shaped holes easily processed. Additionally, cutting certain materials has always been nearly impossible for standard machinery, but with lasers, it is easy to bum, vaporize, or melt away the edges to leave a clean consistent cut. Another benefit is efficiency; for example, the use of laser in processing is faster than traditional industrial methods in say, welding, cutting, and drilling. As a result higher production rates are achievable with laser.

Moreover, since laser processing does not require direct contact between the materials and the equipment, there is no wear nor tear on the tools and there is little down-time. Of course, one of the most important benefits of laser processing is precision. Due to the fact that the positioning of laser beam is computer controlled and that there is no direct contact of the work piece with the laser equipment much higher accuracy is achieved than for any of the conventional equipment. In conventional processes, as tools become worn they also become less precise. That never happens with laser processing - the first cut is as precise as the thousandth cut. The bottom line is that accuracy, cost-efficiency, and flexibility are critical in manufacturing today when saving money and preserving quality are the keys to staying ahead of the game. Laser processing can be the solution that provides all three of those factors. Laser technology can be used in processing of almost all types of materials including the hardest and most difficult to materials. Some of the materials that are easily cut with lasers include super alloys such as Inconel, Waspaloy, titanium and many aluminum alloys.

2-7 Laser Technology in Photovoltaics

When it comes to laser technology, photovoltaic industry has not been left behind and most of the numerous processes in cell manufacturing and modules assembly use in one way or another laser technology. The involvement of laser systems depends on the type of the initial material, crystalline or polycrystalline silicon or thin film solar cells et cetera.

Here our emphasis will be on silicon crystalline solar cells and on laser welding/soldering of solar cells in panel assembly, because contrary to well established laser processes like laser cutting and scribing of cells , laser welding/soldering is still under investigation in many photovoltaic research institutions (Hendel, 2012).

2-8 Application of Laser Technology

In the solar industry, lasers are positioned to have a very large impact on the manufacturing cost, by increasing cell efficiency, improving throughput, and providing manufacturing equipment with low cost-of-ownership. Inherently a non-contact process, lasers provide a clear advantage over competing technologies as wafer thicknesses decrease (220 to 100 microns) and wafer sizes increase (150 - 200 mm) over the next few years. Lasers have low utility requirements and provide an ideal choice for manufacturing equipment as solar production-lines themselves become more environmentally-friendly. As the manufacture of solar cells, from the sand raw material to assembled panel modules is a long and sophisticated industrial process, lasers surely have found use- in many steps of the process and are indispensible tool for the success of the industry their use expand day by day. (Colville, 2012- Bootch, 2010)

A. Edge Isolation

One of the traditional laser applications is edge isolation. The p-doped wafers are coated with an outer layer of n-doped silicon to form a large area p-n junction. This thin (10-20 microns) layer coats the entire wafer, including the edges,- and often the rear surface, creating an unacceptable recombination pathway between the front and back surfaces. This pathway can be eliminated by edge isolation, whereby a groove is continuously scribed completely through this n-type layer. In order to maximize cell active area and hence efficiency, this groove has to be as narrow and as close to the edge as possible. For this purpose the usual laser of choice is a Q- switched diode-pumped solid state (DPSS) laser with a pulse repetition rate around 30 kHz. Some manufacturers use 1064 nm lasers: however, an increasing number of manufacturers .are utilizing 532 and 355 nm lasers for this application (Assets, 2012) due to several reasons.

First - these shorter-wavelength green / UV lasers can scribe narrower grooves. In addition, 1064 nm lasers can create microcracks that emanate from the scribed groove and which, if reaching the edge of the wafer, can compromise structural integrity - this limits how close the 1064 nm-machined trenches can be placed to the edge of the wafer. The 532 and 355 nm lasers give an additional advantage of generating less heat affected zone, HAZ, compared to IR lasers. But fiber lasers are catching in: 20 W (average output power) Q-switch ytterbium pulsed fiber laser (YLP) lasers are being be used for scribing edge isolation grooves at a high speed (2 m/sec or faster). The use of the 532-nm wavelength (frequency doubled) results in a somewhat reduced scribing speed and increased cost but yields scribes with much reduced crystal damage resulting in potential higher yield.

B. Drilling Vias

A simple solar cell has front and back contacts for the charge carriers and the front metal contacts cover a significant area of the cell (5-7%) and thereby reducing the cell efficiency by obscuration of the sun light. To increase the efficiency and power from each module, newer technologies such as “Metal Wrap Through” (MWT) and “Emitter Wrap Through” (EWT) are being implemented where in the front contacts are moved to the back surface, leaving the front surface nearly free of metal obscuration. To connect the front surface of the cell with the back surface, drilling hundreds of small holes or vias in the wafer is part of the solution. A 20 W Q-switch fiber laser is used to drill 50 micro diameter holes in 250 micron thick wafers at a speed of 100-200 holes/sec. For laser drilling of the vias processing throughput can be optimized depending on the wafer thickness and the hole density. To achieve the throughputs required for this application, 1064-nm fiber lasers offer the best combination of peak power, pulse energy and higher pulse repetition rate compared to a 532-nm laser (Alphonse, 2012).

C. Front Surface Contacts

Buried electrical contacts represent one approach to minimizing the area obscured. This is called “Laser Grooved Buried Contacts”, or LGBC method. After the surface has been antireflection-coated with silicon nitride, lasers can scribe narrow surface grooves which are then plated. This results in electrodes with a high volume and collection surface, relative to their width. The grooves have a width and depth of 20-30 microns and are cut at 2-3 mm intervals along the cell. In a recent adaptation of this approach, lasers cut only through the AR coating, and the exposed semiconductor is electroplated. It remains to be seen if ‘next-generation’ front- surface contact methods will bypass LGBC into mass production within the solar industry (Kyeong, 2009),(Heasman, 2007).

D. Laser Fired Contacts

With thinner wafers, it can be electrically and thermo- mechanically advantageous to include a passivation layer between the rear surface aluminum electrode layer and the silicon: however, this passivation layer is non-conducting. The Laser Fired Contacts (LFC) technique, recently developed by Fraunhofer ISE, provides a means through which lasers create localized contacts. At each site, a 1064 nm laser pulse drives the aluminum through the passivation layer and several microns deep into the silicon, creating a localized A1 / Si alloy. Similar to the LGBC method above, the transition from research to mass production has yet to be realized within the industry (Devenport, 2008),(Ortega, 2012),

E. Cutting Wafers

Due to silicon foundry shortages and associated high material costs, manufacturers are moving towards using thinner wafers (100-200 microns). As the wafers get thinner, it is challenging to cut them with conventional mechanical tools which induce micro cracking and ultimately reducing the strength of the wafers. Lasers, offering a non-contact process, have been successfully implemented in production lines to cut wafers. The Q-switched solid-state lasers, with 50-100 ns pulse and peak power up to 20 kW, are used to cut these thin wafers in multiple passes. The Q-switch fiber lasers offer economical and the cleanest process to cut these wafers as secondary process such as chemical etching (often necessary for other competing technologies) are completely eliminated.(Booth, 2010),(Naeem, 2011), Problems related to mechanical and thermal stress due to laser cutting of silicon wafers are well documented for example in (jklasers, 2011).

F. Wafer Marking

To provide traceability throughout the industry-standard 20-25 year cell / module warranty period, long-term identification of the cells is essential. An emerging application for lasers involves ‘soft’ marking on the surface of the wafers. For this application, the ID mark should be clearly visible, while not causing any notable decrease in efficiency over the required lifetime of the cells / modules (Leone, 2010).

G. Laser Surface Texturing

Surface texturing plays a critical role in silicon solar cell performance, affecting both reflectance and light trapping. Moncrystalline cells are typically textured using an anisotropic alkaline etch to create surface pyramids, while multicrystalline cells are textured using an isotropic acid etch resulting in a “scalloped” surface. Other methods include plasma surface texturing (Liu, 2011). An alternative surface texturing technique uses ultrafast lasers that offer advantages over the standard wet etching techniques.

Laser texturing process provides an efficiency improvement and tighter efficiency binning for multicrystalline cells compared to a high quality isotexture baseline, and also maintains high efficiencies on thinner wafers due to superior light trapping. The combination of these benefits directly translates into reduced $/WP cell manufacturing cost. Laser texturing technique using ultrafast; laser (Waver, 2010), (Ruby, 1999) or Q-switched Nd: YAG laser (Vineis, 2010) also holds promise to achieve better performance and economics on monocrystalline cells than standard alkaline etches. Research shows that laser surface texturing with can b‘e efficiently achieved on multicrystalline as well as on monocrystalline solar cells. Using an ultrafast laser processing technique it is possible to create self-assembled micro/nano structures on a silicon surface for efficient light trapping. Light reflection (including scattering) of the Si

surface can be reduced to less than 3% for the entire solar spectrum (Lyengar, 2010)

2.9. Light Management in Silicon Solar Cell

In a solar cell, one major task is to make sure that as much as possible of the incoming sunlight is converted into electricity. In order to achieve this, optical losses must be reduced as much as possible. The effort of reducing these losses is termed light management. Figure 2.15 shows a sketch of possible optical losses in a silicon solar cell, denotes the front surface reflection, which consists of the light being reflected off the front surface without entering the solar cell, denotes the escape light, light which has entered the solar cell, but is able to escape before being absorbed. Three parasitic absorption mechanisms, absorption that does not generate current in the solar cell, are also indicated. Denotes optical absorption in an imperfect rear mirror, free-carrier absorption, is the absorption by conduction band electrons, an optical absorption mechanism which does not generate electron-hole pairs. This mechanism is intrinsic to silicon, and is strongest in highly doped silicon, such as in the emitter. Also the antireflection coating may absorb some of the incident light, here denoted as AArc [Thorstensen, 2013].

With a quite high index of refraction, bare silicon reflects on the order of 30 % of the incoming sunlight due to Fresnel reflection. In order to reduce, two tricks are normally applied. Firstly, an anti-reflection coating can be applied to the surface, consisting of a transparent layer with a thickness of /4 and an index of refraction ideally equal to , thus minimizing or eliminating reflection at the target wavelength, and significantly reducing overall reflection. (For an introduction to Fresnel and thin-film optics, see e.g. (Lyengar, 2010). Typically, when weighting the reflectance spectrum with the AM1.5 spectrum, integrating over a 300 – 1200 nm wavelength range, an integrated reflectance of around 10 % can be achieved by application of an anti-reflection coating. Secondly, texturing of the surface may further increase the optical coupling into the silicon. If the light experiences multiple bounces off the silicon surface, each bounce will reduce the total reflectance.

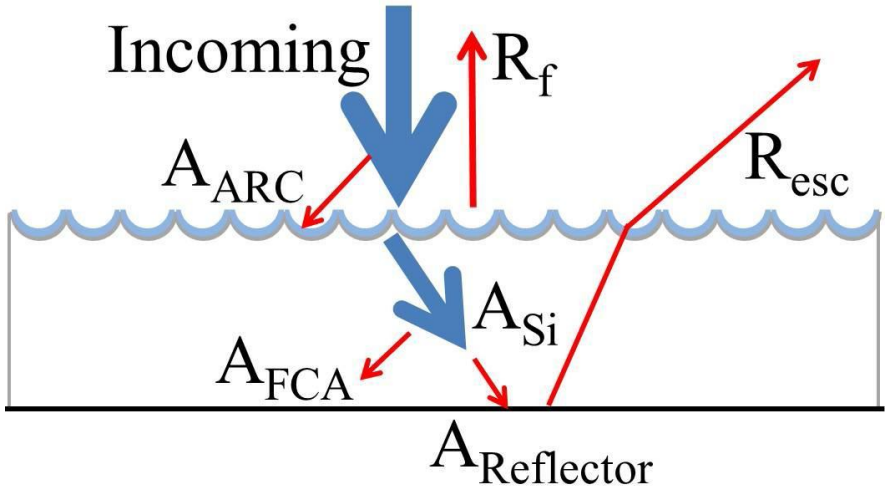

Fig 2.15: Sketch of a wafer showing various contributions to optical absorption and loss in a solar cell. The rear reflector is shown in black, while the anti-reflection coating is shown in blue. ASi denotes the silicon absorption, the only absorption mechanism generating electron-hole pairs. The optical loss is divided into front side reflectance, Rf, escape light, Resc, absorption in the rear reflector, A Reflector, absorption in the AR-coating, AARC, and absorption by free carriers, AFCA.

Silicon is an indirect band-gap semiconductor, meaning that the optical absorption process must be assisted by absorption or emission of a phonon for momentum conservation. This characteristic makes silicon a rather poor optical absorber. While other solar cell materials may show acceptable absorption in a 1 μm thick absorber, silicon requires quite long absorption lengths. This trend is especially clear for photon energies near the band-gap energy of silicon.

In Figure 2.16 (left), the attenuation coefficient and optical penetration depth in silicon is shown. The optical penetration depth is defined as the distance the light has to travel through silicon in order to be attenuated to 1/e intensity level. The hatched range is a range of penetration depths ranging from 160 μm to 20 μm. 160 μm is around the current industry standard wafer thickness, while 20 μm corresponds to a realistic long-term target thickness. It is seen that wavelengths above approx. 800 nm will have the possibility to penetrate the thinnest of these wafers; the penetration depth easily reaches several millimeters at wavelengths above 1100 nm, meaning that the light can travel much further than the thickness of the wafer before being absorbed. It is at wavelengths showing a penetration length on the order of, or longer than the thickness of the wafer that contributions to *Resc* are expected. In order to reduce loss contributions from *Resc*, the path length of the light through silicon must be increased. The act of increasing the path length is often called light trapping. Fig 2.16 (right) shows the photogenerated current, generated from band-to-band absorption by sunlight (AM1.5)(Air mass 1.5 Standard Solar Spectrum) passing through a given path length in silicon. Optical losses occur even to optical path lengths exceeding 1000 μm.

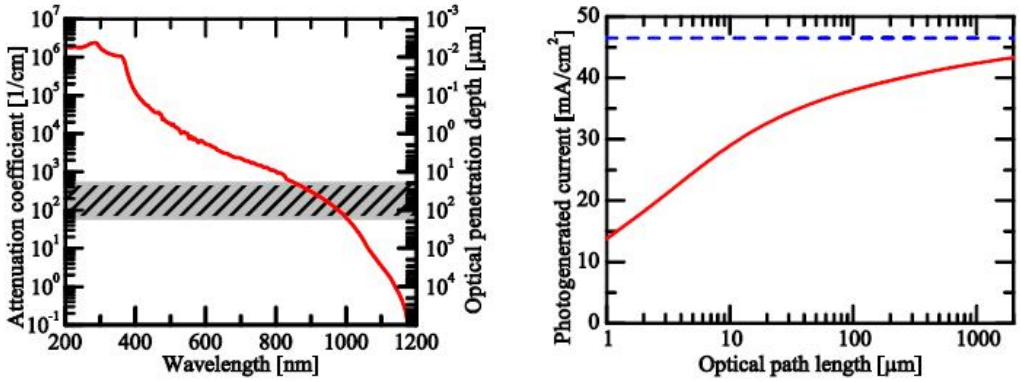

Fig 2.16: Left: The optical attenuation coefficient and corresponding optical penetration depth in silicon as function of wavelength. Also indicated is a relevant range of wafer thicknesses for solar cell applications. The need for light-trapping for wavelengths above 800 – 1000 nm depending on wafer thickness is obvious. Right: The photogenerated current from sunlight (AM1.5) absorbed by a given path length in silicon (solid line). Also indicated is the maximum current available (dashed line) Data taken from ref. (Palik, 1998)

Fig 2.17 shows a collection of light-trapping strategies. A shows planar silicon slab with no rear reflector, where the light gets only one straight pass through the wafer. This must be considered as an absolute worst case scenario. B shows a planar structure with a rear reflector, ensuring two straight passes through the wafer. In a solar cell, the rear metal contact often acts as a mirror (although not a perfect one). C shows a front side textured structure, where the path length in the silicon is increased as a result of the oblique angle taken by the light passing through the wafer. A high probability of escape after two passes is indicated. In silicon, any light hitting the silicon / air interface will be totally.

Internally reflected if the incidence angle is larger than = sin , which for silicon in air, at wavelengths near the band-gap equals approx. 16.5°, a fairly shallow angle. Angles below 16.5° are referred to as the escape

cone, as light within this cone will have a high probability of escaping the silicon wafer.

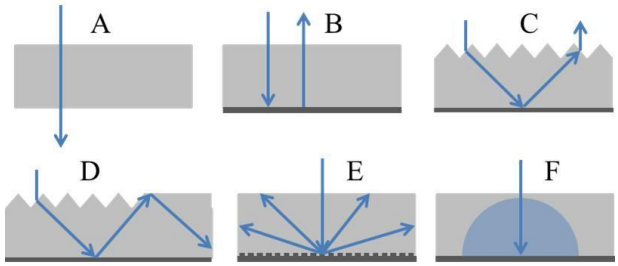

Fig 2.17: Sketch of various light-trapping schemes. A - no light trapping, B - rear reflector, C – front surface texture, D – symmetry-breaking front side texture, E – diffractive rear reflector, F – Lambertian rear reflector.

D and E are examples of more advanced light-trapping structures. In D, a textured surface is shown, but unlike C, the symmetry of the texture is broken. Created correctly, such symmetry-breaking structures can cause most of the light to hit the wafer surfaces at angles outside the escape cone, thereby causing total internal reflection to be dominant, and multiple passes are ensured for the majority of the light. E is meant to indicate a diffractive rear reflector, where the incoming light is diffracted into several diffraction orders. The angle of the diffraction orders can be tuned by varying the grating period so that total internal reflection is ensured for all but the specular diffraction order. If, in addition, the specular order is suppressed, the light trapping can be very efficient. F is meant to indicate the case of Lambertian light trapping. Lambertian light trapping is an idealized theoretical light-trapping scheme, where a perfect rear reflector reflects the light homogenously in all directions, independent of the angle of the incoming light. It can be shown that the Lambertian light trapping is the maximum achievable light trapping for a sample uniformly illuminated from all directions. The path length of light in a Lambertian light-trapping scheme can be calculated to 4 (Lyengar, 2010), where the refractive index of the material and w is the wafer thickness. In silicon, this path length enhancement 4 is about a factor 50.

While light-trapping is not critical in thick wafers, Figure 2.16, (right) shows that thinner wafers benefit strongly from light-trapping. Increasing the path length in a wafer from 20 μm by the Lambertian factor to 1000 μm would increase the photogenerated current from around 70 % of the available photocurrent to above 90 %.

The industry standard for mono-crystalline silicon texturing is today the double sided random pyramid structure. This is created by etching a <100>-oriented silicon wafer in a diluted KOH solution, often adding an alcohol for improved quality of the texture. Such an etch preferentially exposes the <111> crystal planes, leaving a random pattern of upright pyramids. This texture shows a low front surface reflectance, due to the steep angles of the pyramids, and also shows very decent light trapping, as there will be a strong randomization of the direction of the light when refracted or reflected off the various pyramid facets. For multi-crystalline silicon, the random pyramid texture is less efficient, as the direction of the pyramids is dependent of the crystal orientation of the wafer.

Therefore, for multi-crystalline wafers or mono-crystalline wafers with e.g. a <111> orientation, isotropic acidic etching is normally applied. This texture will form random dimple-like structures. As the dimples are generally flatter than the pyramids, the chance of experiencing multiple bounces off the front surface is limited, and the front surface reflectance is significantly higher than for the random pyramids. The light-trapping properties, however, are rather good.

Common for both of these textures, is that they require some form of seeding or attack points in order to form uniformly. Such seed points are readily available today, as most wafers are cut by wire sawing, where the saw damage generates seed points. However, several new wafering technologies are emerging, where no saw damage is present. This poses a challenge for the traditional texturing methods. Furthermore, wafer

thickness is expected to decrease, caused by a need to reduce silicon consumption and silicon costs. The traditional texturing methods will remove significant wafer thickness, being less suitable for thin wafers. To overcome these hurdles, new texturing methods must be developed. This thesis presents two ways of creating light management structures on silicon by laser assisted methods.

2.10 State of Laser Texturing

Already, several approaches to laser texturing of silicon exist. These will be briefly reviewed, and a motivation is given for the approach to laser texturing taken in this thesis.

2.10.1 Black silicon

So-called black silicon can be created by irradiation of a silicon surface using ultra short laser pulses. If a single spot is irradiated by multiple pulses, self-assembling structures tend to emerge, shown in Fig 2.18 (left) (Nayak, 2011). Such structures are often created in a sulfur hexafluoride (SF6) – atmosphere, but they may also be created in air (Bonse, 2002). Black silicon, as the name suggests, displays an extremely low reflectivity over the whole relevant wavelength range, and is as such very close to the ideal anti-reflection coating. On the more practical side, one obstacle seems difficult to bridge. In articles describing black silicon formation, typical parameters may be: Pulse energy density 0.9 J/cm^2, repetitions 300 (Goetzberger, 1998). Using these numbers and multiplying by the size of a 5 inch wafer, total laser energy of around 44 kJ is required. In current production, 1 wafer/second (or more) is the benchmark for a relevant process. In order to deliver 44 kJ of energy to a wafer in such a short period of time, one would need a 44 kW laser. Not only are such lasers far away from state of the art, but even if one could find such a laser, it would be very interesting to see how a silicon wafer would react to such a violent energy input. With very little material

removal, the majority of the laser energy must remain in the silicon wafer. Using the heat capacity and melting enthalpy of silicon, 44 kJ is the energy required to heat and melt a 5 inch wafer with a thickness of around 350 μm. Another issue when working with black silicon in general is the very large surface area that is created. The passivation of such a surface must be of very high quality in order for surface recombination not to be a serious problem. Passivation of black silicon surfaces by the use of atomic-layer deposited Al2O3 is showing promising results (Repo, 2013).

2.10.2. Laser Drilling

A second option for laser texturing is simply to drill a suitable geometric structure, such as the honeycomb structure in mc-silicon shown in Figure 2.18 (middle) (Abbott, 2006). Holes are drilled, and thereafter, the structure is etched in order to remove the laser damaged areas and debris from the process. While this process significantly reduces front surface reflectance for mc-silicon, material removal by laser ablation is an energy intensive process. In this case, 10 J/cm^2 and 3 repetitions were applied. Assuming effective area coverage of 25 % (the 10 J/cm^2 would not be applied to the whole surface), the required energy for texturing of a 5 inch wafer is around 1 kJ. While this is much better than what was the case for black silicon, and in a range where industrial lasers do exist, this is still quite a lot of energy to put into a wafer within one second.

2.10.3. Masked laser processing

A third option for laser processing is masked laser processing, shown in Figure 2.18 (right) (Morikawa, 2010). Here, a SiNx etch barrier has been applied to the wafer, and the laser is applied only for creating openings through the barrier. A wet-chemical etch (in this case an isotropic etch) is applied for material removal and structure development. By this approach, the laser does virtually no material removal, and much lower

laser energy can be applied. Typical pulse energies required for silicon nitride removal is around 0.7 J/cm^2. With an area coverage of around 10 % (the image shown has an area coverage of around 5 %), the energy required for opening the etch barrier on a 5 inch wafer is around 10 J, corresponding to a 10 W laser for 1 wafer / second. This is indeed feasible laser power, and easily available today. This masked approach also uses a diffractive optical element (DOE) in order to create several openings through the etch barrier per laser pulse. This relaxes the demand for accurate, high speed scanning and high repetition rate lasers. The requirements on pulse energy rise with the number of spots per pulse, but lasers tend to have pulse energies easily allowing for a high number of simultaneously processed holes.

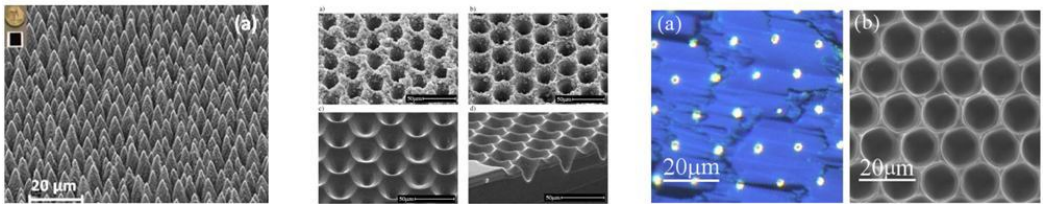

Fig2.18: Images of black silicon structure (Nayak, 2011) (left), laser drilled texture (Abbott, 2006)(middle) and masked texture with etching (Morikawa, 2010) (right).

CHAPTER THREE

EXPERIMENTAL PART

3.1 Introduction

This chapter presents the experimental part of this work, material used and their specifications, setup arrangement and experimental procedure. Laser treatment to irradiation processes of the photovoltaic solar cells in two dimensions (1×1 cm^2, 2×2 cm^2 and 3×3 cm^2)

3.2 Experimental setup

Figure (3.1) shows schematic diagram of the setup used to study the IV characteristic curve of the solar cell.

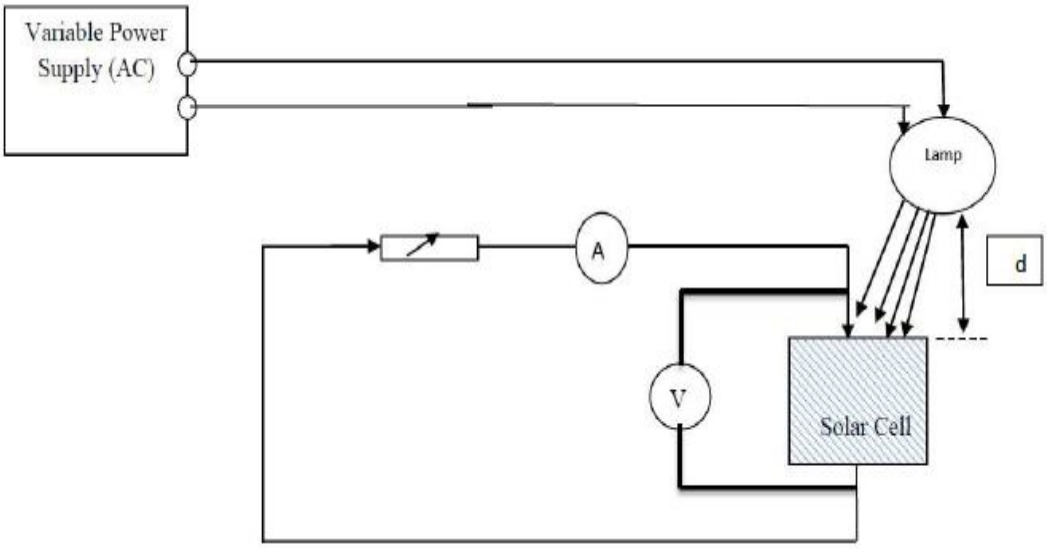

Fig.3.1: Experimental Setup for Solar cell (with & without surface texture) IV curve Measurements

3.3 Material used

The materials used to complete this work, and their specifications are given here:

3.3.1: Auto transformer (Variac)

An autotransformer has a single winding with two end terminals, and one or more terminals at intermediate tap points, or it is a transformer in which the primary and secondary coils have part or all of their turns in common. The primary voltage is applied across two of the terminals, and the secondary voltage taken from two terminals, almost always having one terminal in common with the primary voltage. The primary and secondary circuits therefore have a number of windings turns in common (John winders, 2002).Since the volts-per-turn is the same in both windings, each develops a voltage in proportion to its number of turns. In an autotransformer part of the current flows directly from the input to the output, and only part is transferred inductively, allowing a smaller, lighter, cheaper core to be used as well as requiring only a single winding (K Thayalan,2014). However the voltage and current ratio of autotransformers can be formulated the same as other two-winding transformers:

$$\frac{V_1}{V_2} = \frac{N_1}{N_2} = a$$

($0<V_2<V1$)

Autotransformer 220 AC volts used in this work were supplied from Miken Electronics Ltd, UK in 2000.

3.3.2 Variable resistance

Is a device that is used to change the resistance according to our needs in an electronic circuit? It can be used as a three terminals as well as a two terminal device. Mostly they are used as a three terminal device. Variable resistors are mostly used for device calibration (Circuits today, 2011).

Variable resistor (50 Ω) was used in this work as a two terminal to vary the amount of current passing through the solar cell.

3.3.3 Tungsten lamp

Tungsten lamp is an electric light which produces light with a wire filament heated to high temperature by an electrical current passing through it, until it glows. The hot filament is protected from oxidation with glass or quartz bulb that is filled with inert gas or evacuated. Figure (3.2) shows the construction of the tungsten lamp (Wikipedia, 2015).

The tungsten lamp used in this work was manufactured by with specifications listed in table (3.1).

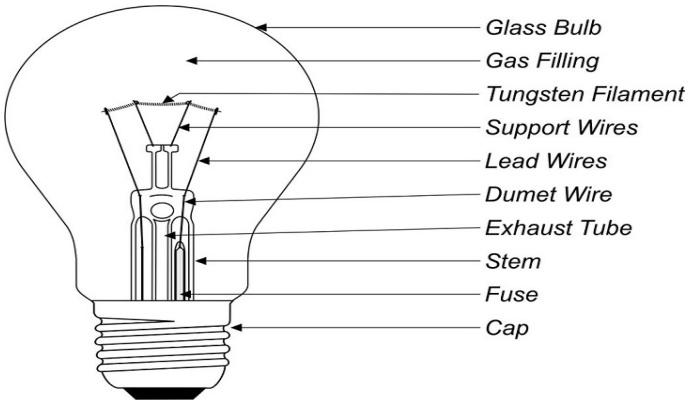

Fig.3.2 Typical incandescent lamp construction

Table 3.1: Specifications of tungsten lamp

Power	100 W
Voltage	130 V
Life hours	10,000
Lumens (Initial)	950
Bulb Color	Frosted
Bulb shape	A19

3.3.4 Digital millimeter

This are the most useful devices which are able to measure voltage and current a.c. or d.c. and the value of capacitance of the capacitor also can be used to measure the value of the resistance of a conductor, also it can be used to measure the temperature of a system through a small probe, furthermore it can be used to check the break of a wire so it is a compact measuring instruments. Its Operation requires a 9 V battery MASTECH MY62 device. And for each of the above measurements a wide range is covered. Two piece of this device was used; one set as (DC) Voltmeter and the other was set as (DC) Ammeter to measure the voltage and current produced from the incident light by the solar cell respectively.

3.3.5 CO_2 (130 W) pulsed laser

The CO_2 laser is a gas laser emit in the Infra-red region of the electromagnetic spectrum the active medium is the CO_2 molecules and as the most gas lasers CO_2 lasers are electrically pumped. CO_2 used in this work was supplied from Flying Technology Development Limited, Shandong, and China. China leading manufacturer for CO_2 laser cutting and engraving machines the device used can be used for many applications.

Device Features

This laser machine takes CO_2 laser tube as thermal source, it can engrave and cut, thus it is applicable for various industries. It is a greatly economical piece of equipment. The whole machine has stable

performance and easy-operation system, coming with professional software. So it can realize high efficiency and good quality processing effect for various industries.

CO_2 Laser used in this work was manufactured by China with specifications listed in table (3.2).

Table 3.2: CO_2 pulsed laser Specifications

Model	FLC9060
Laser-type	10.6μm CO_2 glass laser tube w/ water-cooling
Laser power	90W/100W/130W
Working area	900 x600mm (35.4 x 23.6 inches)
Max Engraving speed:	0-60, 000mm/min
Max cutting speed	0-36, 000mm/min
Laser output control	1-100% software setting
Location precision	Less than 0.01mm
Highest scanning precision	2500DPI
Operating temperature	0 – 45
Operating humidity	5- 95% non-condensing
Minimum shaping character	English 1.0 x 1.0mm
Graphic format supported	HPGL, BMP, PLT, DST, DXF, and AI ...
Driving system	Stepper(Optional: Servo)
Cooling mode	Water-cooling and protection system
Auxiliary equipments	Exhaust-fans, air-exhaust pipe, air pump, water pump
Controller	DSP
Compatible Software	CorelDraw, AutoCAD, Photoshop, TAJIMA
Slope Engraving	Can be easily designed within the "Grade Engrave" function.
Color separation	Uses color property to set function, speed, and laser power

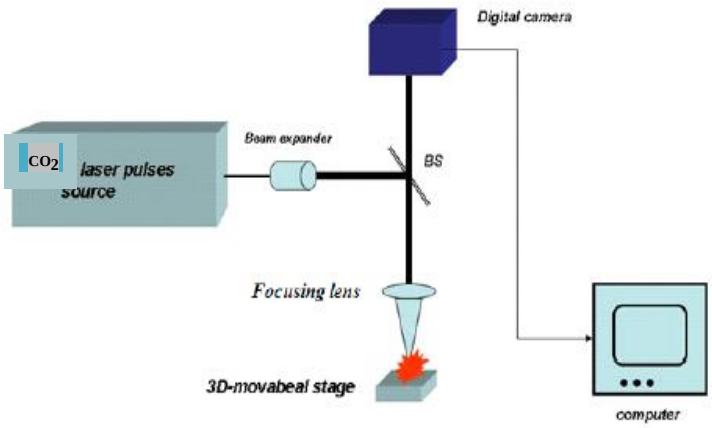

Fig.3.3 schematic diagram of the experimental step of sample irradiation (Taleb, 2011)

3.4 Samples

Solar cells used in this work were assembled by (Nerc-soba solar, 2015) with specifications listed in table (3.3).

Table 3.3: Solar cells samples specifications

Material	Silicon
Area	8X 10 cm^2
Maximum voltage	o.5 volt

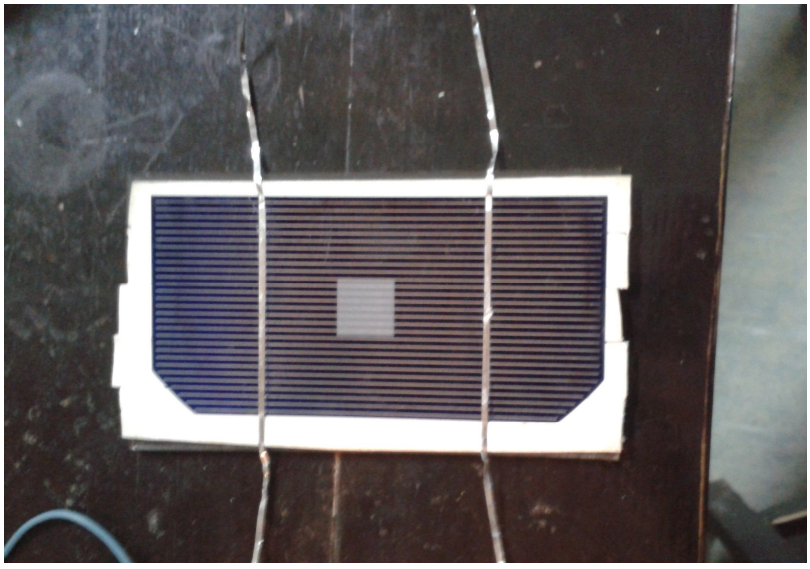

Fig3.4: Solar cell sample

3.5 Setup arrangement

Fig. (3.5) below shows a photograph of the setup arrangement:

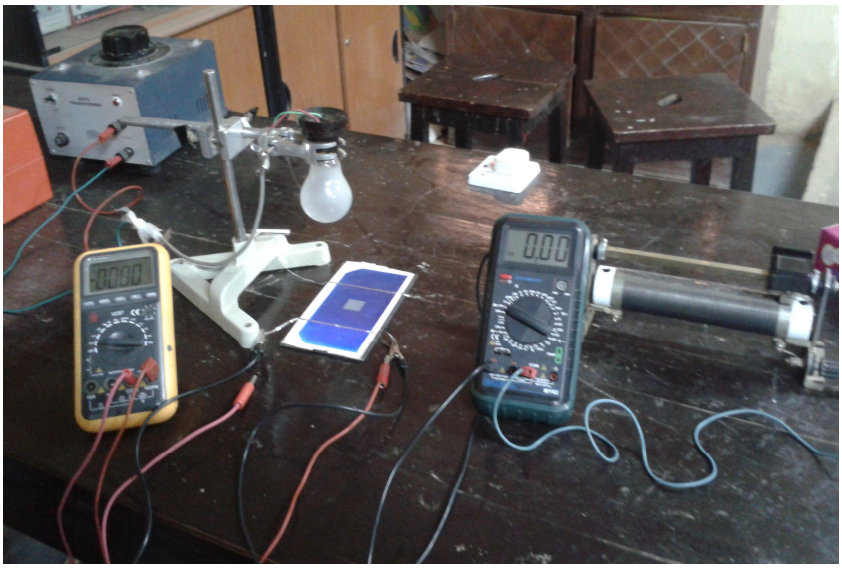

Fig 3.5: Experimental Setup

3.6 Experimental procedure

The procedure was done according to the following sequences:

- The materials were connected as shown in Fig.(3.3)
- The distance from the lamp to the solar cell was carefully measured and control during all measurements.
- The power incident from the lamp on the solar cell was determined by measurement of the lamp current and voltage.
- Solar cell without laser irradiation was used firstly under illuminations with 180 V of the Variac at a distance of 10 cm.
- The obtained results of the two illuminations were tabulated and plotted.
- Solar cells fill factors were calculated according to:

$$FF = \frac{I_m V_m}{I_{sc} V_{oc}} \qquad (3\text{-}1)$$

And the efficiencies were estimated from these values.

$$\eta = \frac{I_m V_m}{P_{light}} = \frac{FF I_{sc} V_{oc}}{P_{light}} \qquad (3\text{-}2)$$

Where FF is the filling factor, I_m & V_m are the maximum current and voltage respectively; I_{sc} is the short circuit current and V_{oc} is the open circuit voltage (all measured under standard conditions. We found the efficiency before & after texturing for solar cells:

- Solar cells were irradiated with CO_2 laser with fixed power 30 Watts and fixed laser scanning speed of 400 mm/s.
- The area of irradiations (surface texturing by cutting number of grooves in centimeters) were varied from 1×1 cm^2, 2×2 $cm^2$and 3×3 cm^2, with 0.1 microns distance of separations and the procedures above were repeated with each solar cell of single area of irradiation.
- The results of IV characteristics curve of the solar cells without irradiation and with irradiations was compared.
- The effect of increasing area of irradiations on solar cell parameters was studied and compared.

3.7 Scanning electron microscopes

- A scanning electron microscope (SEM) is a type of electron microscope that produces images of a sample by scanning it with a focused beam of electrons Fig 3-4. The electrons interact with atoms in the sample, producing various signals that contain information about the sample's surface topography and composition. The electron beam is generally scanned in a raster

scan pattern, and the beam's position is combined with the detected signal to produce an image. SEM can achieve resolution better than 1 nanometer. Specimens can be observed in high vacuum, in low vacuum, in wet conditions (in environmental SEM), and at a wide range of cryogenic or elevated temperatures.

- The most common SEM mode is detection of secondary electrons emitted by atoms excited by the electron beam. The number of secondary electrons that can be detected depends, among other things, on the angle at which beam meets surface of specimen,[citation needed] i.e. on specimen topography. By scanning the sample and collecting the secondary electrons that are emitted using a special detector, an image displaying the topography of the surface is created.

- The SEM was used to study surface texture for photovoltaic solar cells.

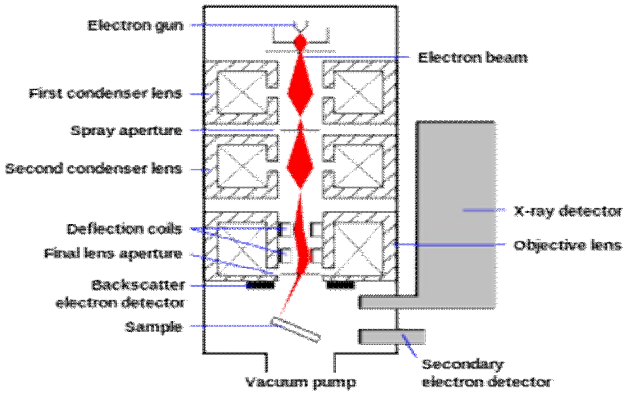

Fig 3.6 Schematic of an SEM.

The results & calculations from this experimental work will be presented and discussed in chapter four

Chapter Four

Results & Discussion

4.1 Introduction

This chapter gives the results of Current-Voltage of the solar cells supported from National Energy Research Center (NERC) - Soba Solar, Sudan (NERC Sudan, 2015), before and after laser surface texturing with the manufacturing features such as dimensions (8×10 cm) and max voltage output of (0.5V). The results of the solar cell after laser surface texturing was carried out with three different areas starting by (1×1 $cm^{2)}$, (2×2 cm^2) and (3×3 cm^2), for each of this textured areas solar cells the IV characteristics according to setup shown in fig (3.2) was measured and the Filling Factor parameter in each case was calculated according to equation in section (3-1) of the experimental procedure, which gives good indication of the solar cell efficiency. Then each Current voltage relation was plotted using Origin Program V.6.

4.2 Results of IV before Laser Texturing

Table 4.1: Current-Voltage of the solar cell before laser texturing

Current (mA)	Voltage (mV)
0.28	0.233
0.25	0.396
0.23	0.438
0.20	0.463
0.19	0.469
0.17	0.48
0.15	0.488
0.14	0.491
0.13	0.493

0.12	0.497
0.11	0.498
0.09	0.502
0.08	0.504
0.07	0.506
0.06	0.508
0.05	0.510
0.04	0.512
0.03	0.514
0.02	0.515
0.01	0.516
0.00	0.517

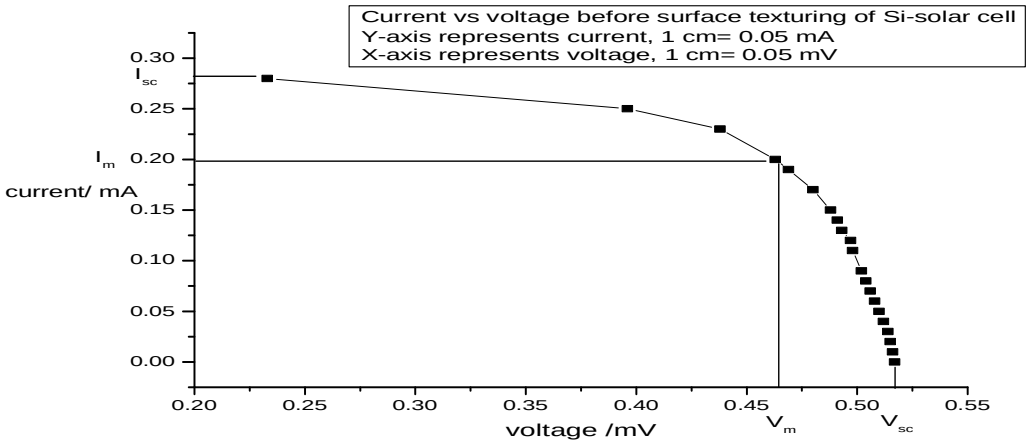

Fig.4.1: The Current-Voltage relation (IV) curve of Si solar cell without laser surface texturing

The results in table (4.1) was plotted using origin program V.6, then a large rectangular inside the IV curve of the solar cell was drawn manually as shown in figure (4.1) above .

The parameters that extracted from the relation shown in figure (4.1) and were used according to this values using equation (3.1) the fill factor is:

$$FF = \frac{I_{\max} V_{\max}}{I_{sc} V_{oc}} = \frac{0.20 * 0.465}{0.52 * 0.28} = 0.638 = \mathbf{63.8\%}$$

4.3 Results of IV after Laser Texturing

The solar cells were textured using CO_2 of 130 W power, the power was tuned to 30 Watts to avoid broken of the solar cells using the device software the speed of scanning of the laser pulses was set to 400 mm/s and the area of textured surface was set for three different solar cells to 1×1 cm^2, 2×2 cm^2 and 3×3 cm^2.

The results in this section were subdivided into three parts:

4.3.1 IV Results of 1×1 cm^2 surface textured area of the solar cell

Since each solar cells are identical in their features we expected that the characteristics are also identical, and then carefully carried out the surface texturing in Khartoum Private company that use a 130 Watts CO_2 pulsed laser with the specifications listed in table (3.2) for decoration process. Using the device software the speed of scanning was set to 400 mm/s and the power set to 30 Watts, and three solar cells were textured each with different area.

After surface texturing again the solar cell was connected to ammeter and the short Circuit current was measured to be (mA) and to a digital millimeter which was set as voltmeter the open circuit voltage V_{oc} was to be (0.53 mV) with the same distance of the tungsten lamp used to obtain the IV characteristics this was measured carefully, and the auto transformer was set to the same values of 160 V ac the same illumination condition, then the circuit was connected as shown in figure (3.2) the rheostat was gradually slides and the values of the voltage and

corresponding current were measured and the results were listed in table4.2.

Table 4.2: Current-Voltage of the solar cell after (1×1 cm^2) laser texturing

Voltage (mV)	Current (mA)
0.155	0.27
0.308	0.26
0.438	0.24
0.453	0.19
0.466	0.17
0.475	0.16
0.482	0.15
0.491	0.13
0.493	0.1
0.495	0.09
0.498	0.08
0.502	0.07
0.508	0.06
0.511	0.05
0.512	0.04
0.514	0.03
0.515	0.02
0.516	0.01
0.516	0

Again results in table (4.2) was plotted using origin program V.6, then a large rectangular inside the IV curve of the solar cell was drawn manually, from the IV curve and the inner maximum

possible rectangular drawn the solar cell parameters those are I_{sc}, V_{oc}, I_{max}, and V_{max} were extracted and then used to calculate the Fill Factor parameter of the given solar cell according to eq. (3.1.). This is illustrated in Figure (4.2) below which shows the IV characteristics of the solar cell before laser surface texturing.

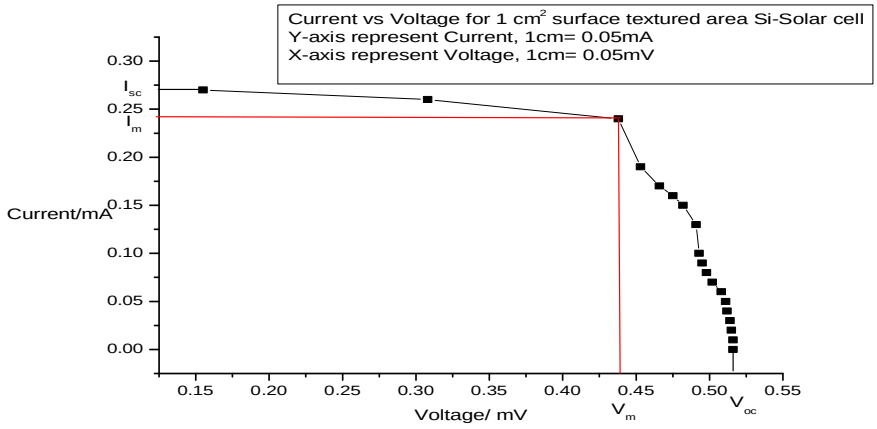

Fig.4.2: The current-Voltage relation (IV) curve of Si solar cell with 1×1 cm^2 laser surface texturing

The parameters obtained from the relation shown in figure (4.2) were:

I_{sc}= 0.27 mA, Voc= 0.52 mV, I_{max}= 0.24 mA, and V_{max}=0.435 mV.

And thus according to this values using equation (3.1) the fill factor is:

$$FF = \frac{I_{max} V_{max}}{I_{sc} V_{oc}} = \frac{0.435 * 0.24}{0.52 * 0.27} = 0.742 = \mathbf{74.2\%}$$

It should mention here that the maximum achievable value of the filling factor for Si solar cell is of about 0.85%.

4.3.2 IV Results of 2× 2 cm^2 surface textured area of the solar cell

For this new textured area, the experiment was repeated and the solar cell was carefully handled in order to avoid damage of the textured surface and with good handling without causes dirty in the solar cell which may results in errors and /or decrease in the current and/or voltages values , then the same procedure of measuring IV characteristics were repeated with the same distance and other laboratories conditions (Such as illumination condition) that exist during that when carrying out the IV characteristics of the solar cell before laser surface texturing . And the obtained results were tabulated in table (4.3).

Table 4.3 results of the I& V of (2×2 cm^2) textured solar surface area:

Voltage (mV)	Current (mA)
0.227	0.28
0.39	0.27
0.43	0.26
0.432	0.25
0.455	0.23
0.465	0.22
0.466	0.21
0.469	0.19
0.472	0.17
0.476	0.15
0.479	0.13
0.481	0.11
0..483	0.09
0.488	0.07
0.491	0.06
0.494	0.05

0.5	0.04
0.504	0.03
0.511	0.02
0.513	0.01

The results in table (4.3) was plotted in figure (4-3) using origin Program V.6 and a large possible rectangular inside the IV characteristics was manually plotted and the interested parameters were identified and extracted, then The Filling factor was calculated using equation (3-1)

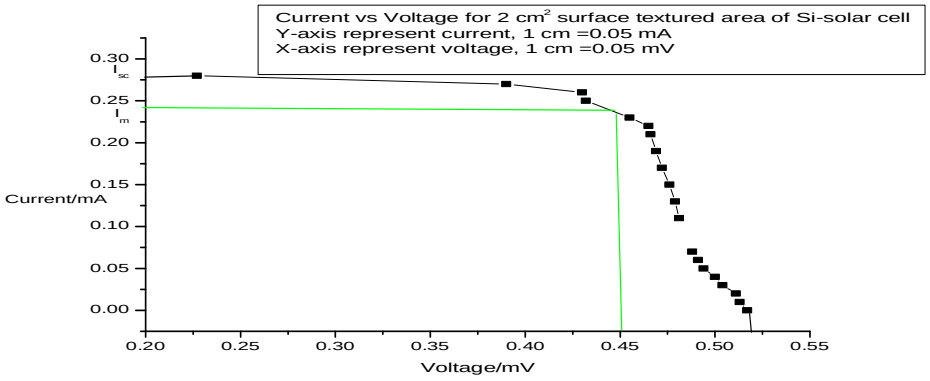

Fig 4.3: Current Voltage characteristics of (2×2cm^2) textured solar cell surface

From this relation the solar cell parameters were found and used to calculate the Fill factor as it did in previous section for either Fill Factor for the solar cell without surface texturing and with (1×1cm^2) surface textured area.

I_{sc}= 0.28 mA, V_{oc}= 0.52 mV, I_{max}= 0.245 mA, V_{max}= 0.45 mV and this value give a FF:

$$FF = \frac{I_{\max} V_{\max}}{I_{sc} V_{oc}} = \frac{0.245 * 0.45}{0.28 * 0.52} = 0.752 = \mathbf{75.2\%}$$

Comparing this with the previous two values of the FF of the solar cell without surface textured and with (1×1cm^2) area of the textured surface, it

is clear that the Filling factor increases rapidly with increasing the textured surface area.

4.3.3 IV Results of (3×3 cm^2) surface textured area of the solar cell

For this new textured area, the experiment was repeated and the solar cell was carefully handled in order to avoid damage of the textured surface and with good handling without causes dirty in the solar cell which may results in errors and /or decrease in the current and/or voltages values , then the same procedure of measuring IV characteristics were repeated with the same distance and other laboratories conditions (Such as illumination condition), that exist during that when carrying out the IV characteristics of the solar cell before laser surface texturing . And the obtained results were tabulated in table (4.4).

Table 4.4 results of I & V of (3×3 cm^2) textured solar surface area:

Voltage (mV)	Current (mA)
0.165	0.28
0.318	0.27
0.449	0.25
0.453	0.23
0.466	0.21
0.475	0.2
0.482	0.19
0.491	0.15
0.493	0.13
0.495	0.12
0.498	0.11
0.507	0.09

0.509	0.07
0.512	0.06
0.513	0.04
0.516	0.03
0.517	0.02
0.519	0.01
0.52	0

The results in table (4.4) was plotted in figure (4-4) using origin Program V.6 and a large possible rectangular inside the IV characteristics was again manually plotted and the interested parameters were identified and obtained, then The Fill factor was calculated using equation given in experimental procedure section (3-7).

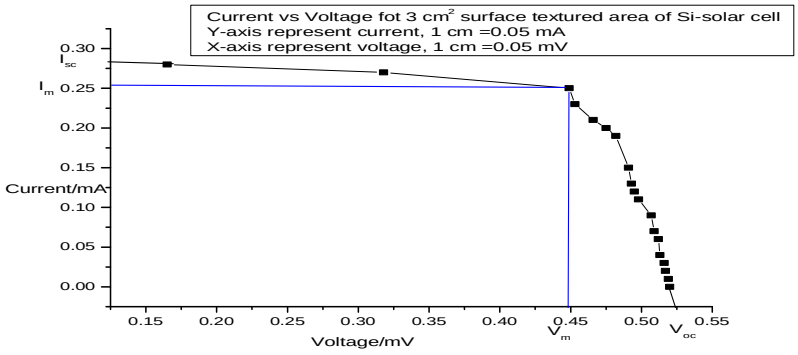

Fig 4.4: Current Voltage characteristics of (3×3 cm^2) textured solar cell surface

From this relation the solar cell parameters were found and used to calculate the Fill factor as it did in previous section for either Fill Factor for the solar cell with and without surface texturing.

I_{sc}= 0.28 mA, V_{oc}= 0.525 mV, I_{max}= 0.255 mA, V_{max}= 0.445 mV

and this value gives a FF:

$$= FF = \frac{I_{\max} V_{\max}}{I_{sc} V_{oc}} = \frac{0.255 * 0.445}{0.28 * 0.525} = 0.768 = \mathbf{76.8\%}$$

Comparing this with the previous two values of the FF of the solar cell with surface textured of ($1\times1 cm^2$ and $2\times2\ cm^2$) areas, it is clear that the Filling factor increases rapidly with increasing the textured surface area.

Another measurement

4.4 Efficiency

The conversion efficiency is the most important property of a solar cell it is defined as the ratio of the photovoltaically generated electric output of the cell. From equation (3-2)

$$\eta = \frac{I_m V_m}{P_{light}} = \frac{FFI_{sc} V_{oc}}{P_{light}}$$

Where FF is the filling factor, I_m & V_m are the maximum current and voltage respectively; I_{sc} is the short circuit current and V_{oc} is the open circuit voltage (all measured under standard conditions. We found the efficiency before & after texturing for solar cells:

4.4.1 Efficiency before texturing

The efficiency of the cell was found before texturing as:

$\eta = \frac{FFI_{sc} V_{oc}}{P_{light}}$ **,** FF= 0.638**,** I_{sc}= 0.28, V_{oc}=0.52 and P_{light} =0.0085

$$\eta = \frac{0.638 \times 0.28 \times 0.52}{0.0085} = 11\%$$

4.4.2 Efficiency after texturing

After texturing the cell efficiency were found as:

a-For the first textured area (1cm × 1cm):

$\eta_{1cm\times1cm} = \frac{FFI_{sc} V_{oc}}{P_{light}}$ **,** FF= 0.742**,** I_{sc}= 0.27, V_{oc}=0.52 and P_{light} =0.0085

$$\eta_{1cm\times cm} = \frac{0.742 \times 0.27 \times 0.52}{0.0085} = 12.25\%$$

b-For the second textured area (2 cm X 2 cm):

$\eta_{2cm\times 2cm} = \frac{FFI_{sc}V_{oc}}{P_{light}}$, FF= 0.755, I_{sc}= 0.275, V_{oc}=0.53 and P_{light} =0.0085

$$\eta_{2cm\times 2cm} = \frac{0.755\times 0.275\times 0.53}{0.0085} = 12.94\%$$

c-For the last textured area (3 cm X 3 cm):

$\eta_{3cm\times 3cm} = \frac{FFI_{sc}V_{oc}}{P_{light}}$, FF= 0.768, I_{sc}= 0.28, V_{oc}=0.525 and P_{light} =0.0085

$$\eta_{3cm\times 3cm} = \frac{0.768\times 0.28\times 0.525}{0.0085} = 13.28\%$$

The above values of the efficiencies clearly increased when the cell is textured moreover increase in the textured area of the cell results in enhancement of the cell efficiency.

4.5 Morphological study of the silicon solar cell with and without laser surface texturing using SEM

Figure 4.5 shows the SEM images of surface structure before (Fig.4.5 (a)) and after CO_2 laser irradiation, it is obvious from the images that surface textures have been formed upon laser treatment. The different textured solar cell surfaces were SEM imaged as figure 4.5 (b) for 1 cm^2, figure 4.5 (c) for 2 cm^2 and figure 4.5 (d) for 3 cm^2.

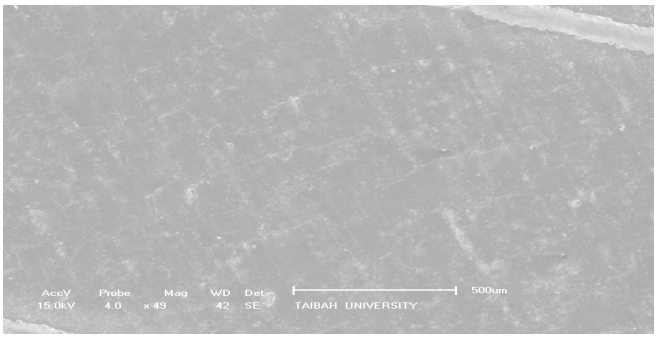

Fig. (4.5.a) SEM image of the cell without texturing

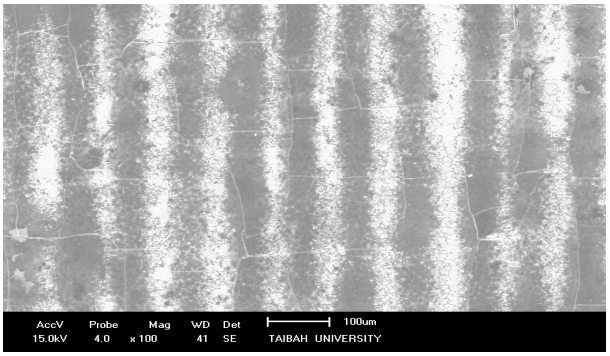

Fig. (4.5.b): SEM image for two dimensional irradiated sample (1x1 cm^2)

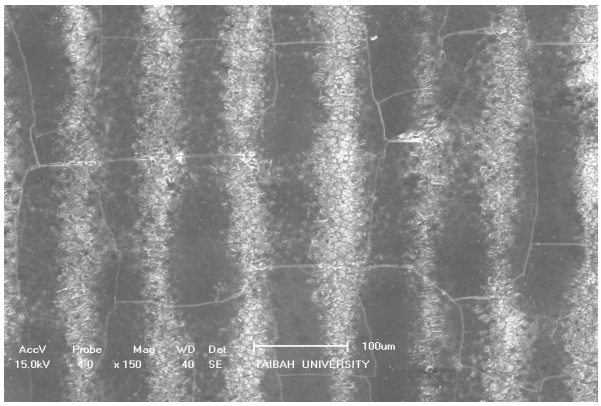

Fig. (4.5.c): SEM image for two dimensional irradiated sample (2x2 cm^2)

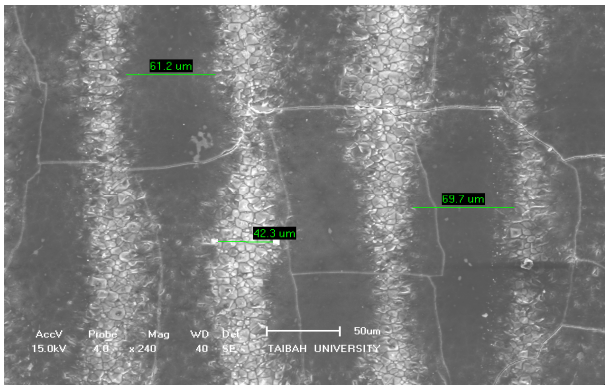

Fig. (4.5.d): SEM image for two dimensional irradiated sample (3x3 cm^2)

Scanning electron microscope (SEM) images of the structures obtained in air environment.

One line scan was performed at affixed scan speed. Aperiodic structure (lines) was formed and observed in nanometre range. The SEM images show a semi periodic structure known as ripples or grooves in submicrostructer and were found after laser irradiation see figures above.

4.6 Conclusions

- In this work the enhancement of the solar cell efficiency was studied via laser surface texturing, for this study different solar cells (with the same features such as materials from which they made, dimension, and output characteristics) were used.

- The voltage-current characteristics of the solar cells at specified distance from tungsten lamp was studied before laser surface texturing and from this characteristics the Fill factor parameter of the solar cell was calculated for the solar cell.

- CO_2 130 watts pulsed laser was used (with 30 Watts power and 400 mm/s speed of scanning) to texture the solar cells and then studied their characteristics after surface texturing, using different solar cells three different areas were textured and the IV characteristics were studied, Fill Factors were obtained and compared with that obtained before laser surface texturing.

- The results of IV characteristics curve of the solar cells without irradiation and with irradiations was compared.

- The effect of increasing area of irradiations on solar cell parameters was studied and compared.

- In conclusion it was found that solar cell efficiency increased as the textured area increased this was clear from the obtained fill factors of the three solar cells with the three different textured areas.

4.7 Recommendations

From the obtained results one can write the following as recommendations:

- Furthers studies for enhancement of the solar cell efficiency via laser surface texturing is recommended.
- Studying the effect of increasing the laser power & pulse duration used for the surface texturing on the solar cell efficiency.
- Studying the surface morphology and solar cell performance after texturing via femtosecond laser could be good technique for taking the PV solar cell specification.
- Studying the effect of texturing on the performance on the polymer solar cells.

References

- Ali A. S.Marouf, Sora F.Abdalah, Wafa S.Abdulrahman and K. Al Naimee, the Role of Photonic Processed Si Surface in Architecture Engineering. Volume 3. USA: Study of Civil Engineering and Architecture 2014.

- Alphonse Niyibizi, Bernard W. Iuka ,Paul N. Kioni and P. K.Kihato, Proceedings of the 2012 Mechanical Engineering on Sustainable Research Innovation, Volume 4,3rd-4th May 2012
- Arnaud Zoubir, Cedric Lopez, Martin Richardson, and Kathleen Femtosecond laser fabrication of tubular waveguides in poly (methyl methacrylate). OPTICS LETTERS / Vol. 29, No. 16 / August 15 2004.
- Arnaud Zoubir, Lawrence Shah, Kathleen Richardson and Martin Richardson. Technology developments towards the practical use of femtosecond laser micro-materials processing. High-Power Laser Ablation IV. Claude R. Phipps, Editor, Proceedings of SPIE Vol. 4760.2002
- Arnaud Zoubir, L.shahk,M.richarson, Practical uses of femtosecond laser micro-materials processing. Appl. Phys. A 77, 311–315, 2003
- B. K. Nayak, V. V. Iyengar, and M. C. Gupta, “Efficient light trapping in silicon solar cells by ultrafast-laser-induced self-assembled micro / Nano structures,” Progress in Photovoltaics: Research and Applications, vol. 19, pp. 631–639, 2011.
- Baum, A. Optical characterization of PMMA phases gratings written by a 387 nm femtosecond laser. Optics Communications 284, 2771–2774, 2011.

- Becker H, five years of operational experience in the German 1000- Roofs-PV Programme - Results of monitoring and system inspection. Proc. 14th European Photovoltaic Solar Energy Conf., Barcelona 1997, p. 1677.
- Becquerel AE, comtRend.Academie.science 9. 1839 p.561.
- Block HD. Wagner G. Proc. 16th European Photovoltaic Solar Energy Conf., Glasgow 2000 p. 1059.
- C. Leone, V. Loprestoa N. Pagano, S. Genna and I. De Iorio, Laser cutting of silicon wafer by pulsed Nd:YAG source Available: http://www.iproms.org/sites/default/papers/Paper_40.pdf
- C. Vineis, M. Levy-Finklshtein, J. Carey, G. Knight, E. Wefringhaus and R.Harney, Ultrafast laser texturing for enhanced solar cell performance and lower cost. Available: http://sionyx.com/pdf/solarcellperformance whitepaper.pdf
- V.V. lyengar, B. K. Nayak and M.C. Gupta, "Optical properties of silicon light trapping structures for Photovoltaics", Solar Energy Materials and solar cells, vol 94, Issue 12, 2010, p.2251-2257
- Ciszek TF, J. Crystal Growth 66 1984 p. 655.
- Craig, B. A. & Piqué, A., Laser Direct-Write Processing. MRS BULLETIN.VOLUME 32. JANUARY 2007.
- D. Kyeong, M. Gunasekaran, K. Kim, H. Kim, T. Kwon, I. Moon, Y. Kim, K. Han and Y. Yi, Laser Edge Isolation for High-efficiency crystalline silicon solar cells , Journal of the Korean Physical Society, Vol. 55 No 1. 2009, p.124-128.
- D.A. Zuev, O.A. Novodvorsky, A.A. Lotin, A.V. Shorokhova, O.D.. Khramova, application of laser texturing method for mc-si solar cells fabrication 2013

- D. M. Kro, W. Chan, T. R. Huser, S. H. Rishud and J.S. Hayden Fs-Laser Fabrication of Photonic Structures in Glass: the Role of Glass Composition. Fifth International Symposium on Laser Precision Micro fabrication, Edited by I. Miyamoto, H. Helvajian, K. Itoh, K. F. Kobayashi, A. Ostendorf, K. Sugioka, Proc. of SPIE Vol. 5662 (SPIE, Bellingham, WA 2004).
- D.S. Ruby, S.H. Zaidi, M. Roy and M. Narayan, Plasma Texture of Silicon Solar Cells in 9th Workshop on Crystalline Solar Cell Materials and Processes, Breckenridge, 1999.
- Dieil D. Helmreich. Siitl E. *Crystals:* Growth, Properties and Applications, Vol. 5. Springer 1981 p. 57
- Dietl J, Helmreich D. Sirtl E. Crystals: Growth, Properties and Applications. Vol. 5. Springer 1981 p. 57
- Dobrzański, L.A. & Drygała, A., Surface texturing of multicrystalline silicon solar cells. Journal of Achievements in Materials and Manufacturing Engineering, VOLUME 31ISSUE1November 2008.
- E. D. Palik, Handbook of Optical Constants of Solids. Elsevier, 1998.
- E. Yablonovitch and G. D. Cody, "Intensity enhancement in textured optical sheets for solar cells," IEEE Transactions on Electron Devices, vol. ED-29, no. 2, pp. 300–305, Feb. 1982
- Erge T et al, The Greman experience with grid- connected PV system, Solar Energy 70, No,6 2001 p. 479-487
- F. Colville, Laser Systems and processes within Next-Generation Photovoltaic Manufacturing Equipment , 4th Photovltaic

Manufacturing Technology Conference, Semicon, Stuttgart, Sept. 2008

- Florea, C. & Kim A. Fabrication and Characterization of Photonic Devices Directly Written in Glass Using Femtosecond Laser Pulses. JOURNAL OF LIGHT WAVE TECHNOLOGY, VOL. 21, NO. 1, JANUARY 2003.

- Gamberale M. Gastello S. Li Causi S, The Italian Roof-Top Program: Status and perspectives. PV in Europe, Rome, Italy 2002 p. 1012 -1015
- Gee JM, Schubert K. Basore PA. Proc. 23rd IEEE Photovoltaic Specialists Conf., Louisville. USA 1993 p. 265
- Goetzberger A, Shockley W. J. Appl. Phys. 31 1960 p. 409
- Goetzberger A. Kleiss G. Reiche K, Nordmann T, Proc. 2nd World Conf. on Photovoltaic Energy Conversion. Vienna, Austria 1998, p. 3481
- Goetzberger A. Knobloch .J. Voss B. Crystalline Silicon Solar Cells. John Wiley & Sons 1998
- Goetzberger A. William Cherry Award Lecture, Proc. 26th IEEE Photovoltaic Specialists Conf., Anaheim. USA 1997 p. 1
- Goetzberger V.U. Hoffmann, Photovoltaic Solar Energy Generation, Springer-Verlag Berlin Heidelberg, Germany 2005.
- Graham, D. M., Martin, A. & Michael, J. W., Direct laser written waveguide–Bragg gratings in bulk fused silica. OPTICS LETTERS/ Vol. 31, No. 18 / September 15 2006.

- Green MA. Prog. Photovolt. Res. App. 7 1999 p. 31.
- H. Booth, Laser Processing in Industrial Solar Module Manufacturing, JLMN-Journal of Laser Micro/Nano engineering Vol. 5, No. 3, 2010, p.183-191

- H. Morikawa, D. Niinobe, K. Nishimura, S. Matsuno, and S. Arimoto, “Processes for over 18.5% high-efficiency multi-crystalline silicon solar cell,” Current Applied Physics, vol. 10, no. 2, pp. S210–S214, Mar. 2010.
- Hezel R. Sol En Mat. Solar Cells 74 2002 p. 25
- J. Bonse, S. Baudach, J. Krüger, W. Kautek, and M. Lenzner, “Femtosecond laser ablation of silicon-modification thresholds and morphology,” Applied Physics A, vol. 74, no. 1, pp. 19–25, Jan. 2002.
- J. Liu, J. Lu, X.Ni, G. Dai, L. Zhang1, Y. Chen, Numerical study on thermal stress cutting of silicon wafer using two-point pulsed laser, Optica Applicata, Vol. XLI, No. 1, p.247-255, 2011.
- J. Thorstensen and S. E. Foss, “Laser assisted texturing for thin and highly efficient monocrystalline silicon solar cells,” in Proceedings of the 26th European Photovoltaic Energy Conference, pp. 1628 – 1631, 2011.
- J. Thorstensen and S. E. Foss, “Temperature dependent ablation threshold in silicon using ultra short laser pulses,” Journal of Applied Physics, vol. 112, no. 10, p. 103514, 2012.
- J. Thorstensen, J. Gjessing, E. Haugan, and S. E. Foss, “2D periodic grating by laser processing, Energy procedia, Vol.27, pp343-348, 2012.
- J. Thorstensen, J. Gjessing, E. S. Marstein, and S. E. Foss, “Light-trapping Properties of a Diffractive Honeycomb Structure in Silicon,” IEEE Journal of Photovoltaics, vol.3, no. 2, pp. 709 – 715, 2013.
- J. Thorstensen, S. E. Foss, and J. Jessing, “Light-trapping properties of patch textures created using Laser Assisted

Texturing," Progress in Photovoltaics: Research and Applications, available online, DOI: 10.1002/pp. 2335, 2013.

- Jostein Thorstensen and Sean Erik Foss, "Investigation of depth of laser damage to silicon as function of wavelength and pulse duration," accepted for publication in Energy Procedia, May 2013.
- Jostein Thorstensen and Sean Erik Foss, "New approach for the ablation of dielectrics from silicon using long wavelength lasers," submitted to Energy Procedia, March 2013
- Jostein Thorstensen, Ragnhild Sæterli and Sean Erik Foss, "Laser ablation mechanisms in thin silicon nitride films on a silicon substrate," submitted to IEEE Journal of Photovoltaics, April 2013.
- JosteinThorstensen, LASER PROCESSING FOR THIN AND HIGHLY EFFICIENT SILICON SOLAR CELLS, PhD thesis Department of Physics Faculty of Mathematics and Natural Sciences, University of Oslo, [online] Available from http// www.mn.uio.no/fysikk/english/people/aca/aas/theses/JosteinThorstensen_PhD_Thesis_final_2jun2013.pdf
- K C Heasman, A Cole, M D Brown, S Roberts, S Devenport, I Baistow, T M Bruton, Development of laser grooved buried contact solar cells for use At concentration factors up to 100x Proc. 22nd EUPVSEC, Issue,: p. 1511-1514, Sept 2007.
- Kais A.Alnaimee IRAQI JOURNAL OF APPLIED PHYSICS Vol.(7), no(2), June 2011.
- Kallepalli, L. N. D. & Desai, N. R., Comparative Study of Defect Formation in Femtosecond Laser Irradiated Polymers and Crystalline Media. Photonics and Optoelectronics (P&O) April (2013) Volume 2 Issue 2. Sons.
- Kaltschmitt M. Wiese A, Erveuerbare Energietrager in Deutschland. Potentiate und **Kosten.** Springer 1993

- Kazuyoshi, ITOH., Laser micro engineering of photonic devices in glass. JLMN-Journal of Laser Micro/Nano engineering, Vol.1, No.1, 2006.
- Knobloch J, Glunz SW. Biro D, Warta W, Schaffer E, Wettling W, Proc. 25th IEEE Photovoltaic Specialists Conf., Hawaii. USA 1994 p. 1477
- Krishnan.R, S. Dash, R.Kesavamoorthy, C. Babu Rao, A.K.Tyagi and Baldev Raj, Laser Surface Modification of Thermal Sprayed Aluminium Oxide Coating. Surface and Coatings Technology, 2006, 2791...
- L.A. Dobrzański and A. Drygała, Surface texturing of multicrystalline silicon solar cells, Journal of Achievements in Materials and Manufacturing Engineering, Volume 31 November 2001
- Laramert MD. Schwartz R.J. IEEE TED 31 1977 p. 337
- Laser cutting of silicon wafers http://www.jklasers.com/images/pdfs/
- Luis A.Fernandes ,Jason R.Grenier,Peter R.Herman ,Stewart Aitchison and V.S .Marques, Femtosecond laser fabrication of birefringent directional couplers as polarization beam splitters in fused silica, Optical Society of America Vol. 19, No.13 /OPTICS EXPRESS 11992 ,2011.
- M. Abbott and J. Cotter, “Optical and Electrical Properties of Laser Texturing for High efficiency Solar Cells,” Progress in Photovoltaics: Research and Applications, vol. 14, pp. 225–235, 2006.
- M. Naeem , Cutting performance comparison between low power LPSS and SM fiber laser for mono and polycrystalline silicon wafers http://www.jklasers.com/images/pdfs/

- Mark L. Brongersma, Yi Cui, and Shanhui Fan, Light management for photovoltaic using high-index nanostructures, nature materials 2014. https://web.stanford.edu/group/cui_group/papers/Cui_NANOMAT_2014.pdf
- Nitsch J. Trieb F, Potenziale und Perspektiven regenemtiver Energietrager. Study for the German Parliament ,March 2000
- Nussbaumer H. Herstellung und Eigenschaften reknstalhsierter Silizium- schichten, Dissertation, University of Konstanz 1996
- O. S. Heavens, Optical properties of thin solid films. New York: Dover Publications, Inc., 1991.
- P. Ortega, A. Orpella, I. Martín , M. Colina, G. López , C. Voz, M. I. Sánchez , C. Molpeceres, R. Alcubilla , Laser-fired contact optimization in c-Si solar cells , Progress in Photovoltaics: Research and Applications, Vol.20, Issue 2, p.173-180, 2012.
- P. Repo, A. Haarahiltunen, L. Sainiemi, M. Yli-Koski, H. Talvitie, M. C. Schubert, and H. Savin, "Effective Passivation of Black Silicon Surfaces by Atomic Layer Deposition," IEEE Journal of Photovoltaics, vol. 3, no. 1, pp. 90–94, Jan. 2013.
- P.Waver, U. Vom Bauer, J. Muller and D.P. Schreiter, Every solar cell is an original: laser marking of silicon solar cells yields new opportunites in quality control , Photovoltaics International, p.16-22, Nov 2010.
- Palm J. Lerchenberger A. Kusian W, Kriihler W. Endros A, Mihalik G, Pickett B. Nickerson. Jester T. Proc. 16th European Photovoltaic Solar Energy Conf... Glasgow 2000 p. 1222
- Patrick Henry Drive, Santa Clara, Laser Systems & Processes within Next Generation Photovoltaic Manufacturing Equipment,

4thPhotovoltaic Manufacturing Technology Conference, Semicon Europa, Stuttgart 2008.

- R. Hendel, B. Lehner and C. Ruttimann, Faster and reliable joining of solar cells bi-wavelength laser welding for photovoltaic module integration, Laser Technik Journal, Vol. 9. Issue 1, 2012, pp. 20-23
- S. Devenport, S Roberts, K C Heasman, A Cole, D Tregurtha and T M Bruton , Process optimization for coloured laser grooved buried contact solar cells 33rd IEEE Photovoltaic Specialists Conference , 2008, p.1-4
- Sakata IT Kawamoto K. Taguchi M. Baba T, Tsuge S, Uchihashi K, Nakamura N, Kivama S, Proc. 28th IEEE Photovoltaic Specialists Conf., Anchorage. Alaska. USA 2000 p. 7
- Schneiderlochner E. Preu R. Ludemann R, Glunz SW, Prog. Photovoltaic. Res. Appl. 10 2002 p. 29
- Sinton RA et al., IEEE Electron Dev. Lett. 7 1986 p. 567
- Spectra Physics, "Laser Edge Isolation Scribing for crystalline silicon solar cell Production". Available: http// assets Newport.com
- Staebier DL, Wronski CR. Appl. Phys. Lett. 31 1977 p. 292
- Swanson RM et al.. IEEE TED 31 1984 p. 661
- Taleb, A. M, K.A AL-Naimee, S.. Abdalah , Riccardo Meucci, F.T Arecchi,. "Nanostructure Formation in Silicon Photovoltaic Cells by Femtosecond Laser Pulses ".Materials Science Forum Vol. 670 pp 118-12 2011.
- Tan, B., Narayanswamy, R. S. & Venkatakrishnan, K., 2005 direct grating writing using femtosecond laser interference fringes formed at the focal point. J. Opt. A: Pure Appl. Opt.7 2005 169–174
- V. Oliveira,N.I. Polushkin, O. Conde, R. Vilar,"nlaser surface pattering using a Michelson interferometer and femtosecond laser radiation", Optics& Laser Technology 44, 2072-2075 2012

- Van Kerschaver E , Proc. 2nd World Conf. on Photovoltaic Energy Conversion, Vienna. Austria 1998 p. 1479
- Vishnubhatla, K.C, S.Venugopal Rao, R.Sai Santosh Kumar,K.Shiva Prasad,P,S.R.Prasad and D.Narayana Rao, Inscription and characterization of micro-structures in silicate, FOTURAN^{TM} and tellurite glasses by femtosecond laser direct writing. Commercial and Biomedical Applications of Ultrafast Lasers VIII, Proc. of SPIE 2008 Vol. 6881.
- Wenham SR. Honsberg CB. Green MA. Sol. En. Mat. Solar Cells 34 1994
- Wilk, H, Grid-connected PV-Systems in Austria, lessons learned. Proc. 17th European Photovoltaic Solar Energy Conf.. Munich 2001 p. 907.